Dynamics and control of a multi-body planar pendulum

Firdaus E. Udwadia & Prasanth B. Koganti

Nonlinear Dynamics
An International Journal of Nonlinear Dynamics and Chaos in Engineering Systems

ISSN 0924-090X

Nonlinear Dyn
DOI 10.1007/s11071-015-2034-0

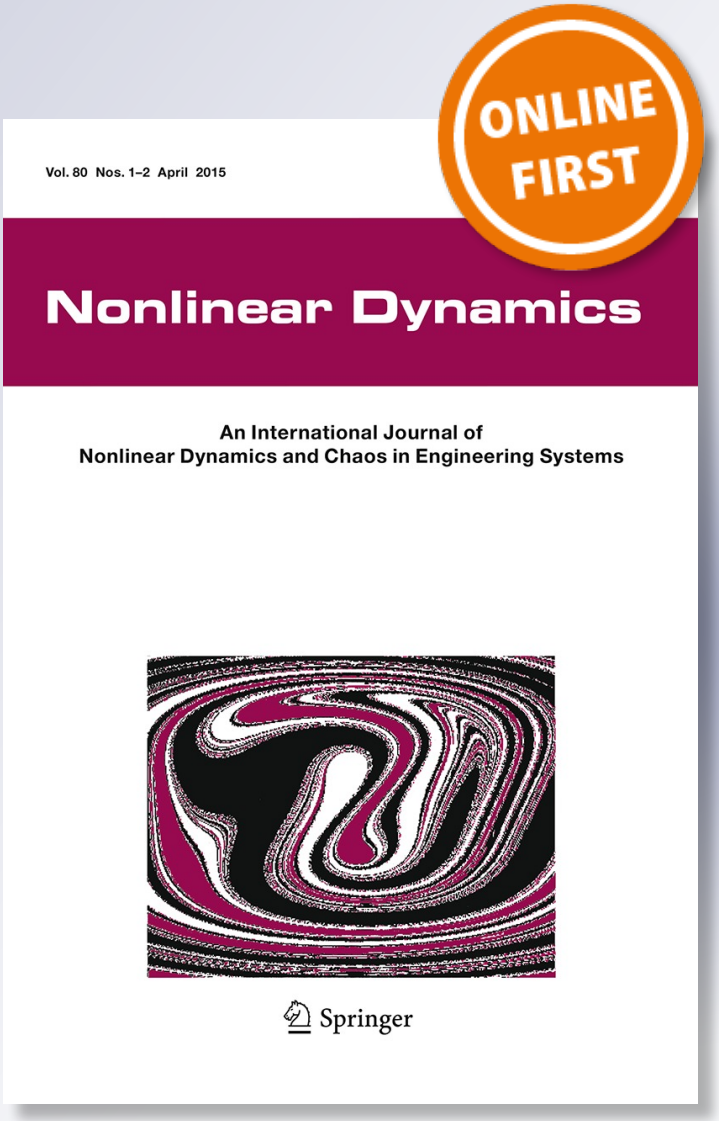

Springer

Nonlinear Dyn
DOI 10.1007/s11071-015-2034-0

ORIGINAL PAPER

Dynamics and control of a multi-body planar pendulum

Firdaus E. Udwadia · Prasanth B. Koganti

Received: 26 September 2014 / Accepted: 13 March 2015

Abstract The explicit equations of motion for a general n-body planar pendulum are derived in a simple and concise manner. A new and novel approach for obtaining these equations using mathematical induction on the number bodies in the pendulum system is used. Assuming that the parameters of the system are precisely known, a simple method for its control that is inspired by analytical dynamics is developed. The control methodology provides closed-form nonlinear control and makes no approximations/linearizations of the nonlinear system. No a priori structure is imposed on the controller. Globally, asymptotic Lyapunov stability is achieved along with the minimization of a user-provided control cost at each instant of time. This control methodology is then extended to include uncertainties in the parameters of the system through the use of an additional continuous controller. Simulations showing the simplicity and efficacy of the approach are provided for a 10-body pendulum system whose model is only known imprecisely. The ease with which the uncertain system can be controlled to move from any initial state to various final so-called inverted configurations is demonstrated.

Keywords N-body pendulum system · Equations of motion · Nonlinear damping · Lyapunov constraint control · Global asymptotic stability · Uncertain systems control · Generalized sliding mode control

1 Introduction

Control of pendulum systems has been at the center of attention of the scientific community for a long time. The reason is that these systems are conceptually simple and can be thought of as useful approximations in the study of several real-life dynamical systems such as two-dimensional robotic manipulators, robot arms, legs of a biped robot, and numerous other articulated mechanical systems. Though conceptually simple, they are highly nonlinear, and inverted pendulum systems, which are unstable, pose significant challenges in control design. For this reason, control theorists often use (inverted) pendulum systems as test beds to test, develop, validate, and compare different control methodologies. Control methods that can successfully stabilize such unstable systems can then be used with greater confidence when applied to other mechanical systems such as those that arise in aerospace engineering, satellite systems, and in the control of general multi-body systems.

F. E. Udwadia (✉)
Department of Aerospace and Mechanical Engineering, Civil Engineering, Mathematics, and Information and Operations Management, University of Southern California, Los Angeles, CA 90089-1453, USA
e-mail: feuusc@gmail.com

P. B. Koganti
Department of Civil Engineering, University of Southern California, Los Angeles, CA 90089, USA

Published online: 29 March 2015

This paper studies the dynamics and control of an n-body pendulum system in which each body comprising the system is planar and of arbitrary shape. The system is more general than that used to date in the literature because the center of mass of each body is not required to lie on the line joining the hinges (see Fig. 1). We refer to such a multi-body planar pendulum with n number of bodies as an n-body pendulum. This paper is conceived in three parts. The first deals with the development of the Lagrange equations of motion for a multi-body planar pendulum. The second part deals with the development of a Lyapunov stable control methodology, which is inspired by some recent results in analytical dynamics, and does not use conventional control theory. It permits the nonlinearly damped pendulum system to start from any given initial conditions and reach a desired final state, hence providing global asymptotic convergence. The third part of this paper deals with the question of controlling an actual physical multi-body pendulum whose description is not precisely known. The control methodology developed in the latter two parts of the paper is applicable to general nonlinear, nonautonomous uncertain dynamical systems. One of the main purposes of the paper is to demonstrate the simplicity and effectiveness of the control methodology in dealing with unstable, multi-degree of freedom systems—in this case, a ten degree of freedom pendulum that is controlled to stably 'stand' in various so-called unstable configurations.

The derivation of the explicit equations of motion for a multi-body planar pendulum, though a seemingly straightforward application of Lagrangian mechanics, can get rather complex when dealing with a pendulum consisting of more than four bodies. In fact, the algebraic complexity explodes as the number of degrees of freedom of the system increase and general equations of motion for n degrees of freedom become extremely unwieldy and long. For example, Refs. [1] and [2] that deal with the development of such equations for an inverted planar pendulum spend several pages deriving the equations of motion, which are then employed for either a two-link or three-link pendulum. References [3] and [4] derive the equations of motion of a similar system—an inverted pendulum with a follower force; they show the considerable degree of algebraic complexity in getting the general equations of motion. Reference [5] presents an algorithm to generate the equations of motion for robotic manipulators automatically using a computer program. The Newton–Euler formalism is used to obtain the equations of motion instead of the Lagrangian formalism. However, the resulting method is still quite cumbersome as seen from the application of this approach to just a double pendulum system [5].

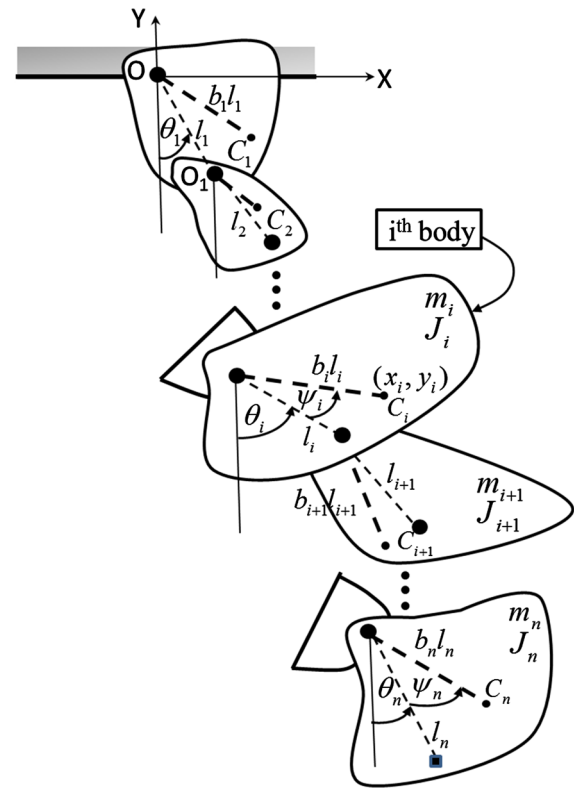

Fig. 1 An n-body planar pendulum. The location of the center of mass, C_i, of the ith body with respect to the inertial coordinate system shown is (x_i, y_i), and the distance between its upper and lower hinges is l_i. The angles θ_i that the line joining the hinges in the ith body makes with the vertical, and the angles ψ_i are measured in the counterclockwise direction, as shown. The location of the lower hinge on the nth body, shown by the *square*, is taken to be any arbitrary point in it, different from the upper hinge

All the equations of motion for pendulum systems obtained to date deal solely with individual links/bodies that are 'straight', i.e., the center of mass of each body (forming the pendulum system) lies on the line joining the hinges in the body (see Fig. 1). In this paper, we present an explicit set of equations in compact form for a more general situation wherein the center of mass of each body (in the n-body pendulum) may lie at a point that is not on the line joining the hinges in that body. To the best of our knowledge, the equations of motion for such systems have not been reported so far in

the literature. More importantly, the derivation of these equations is short and simple and relies on an approach based on mathematical induction on the number of bodies in the pendulum system. The authors are unaware of the use of this sort of approach being applied to get the nonlinear Lagrange equations of motion for an n-body system that has this level of complexity. A significant advantage of the approach (as compared with the direct approach used in Refs. [1–4]) is that the resulting equations are obtained in a compact form so their general structure can then be easily discerned. The equations are then extended to include pendulum systems with nonlinear (and linear) damping. It is these equations of motion of the nonlinearly damped n-body pendulum system that are used in the subsequent sections of the paper.

The second part of this paper deals with the development of a Lyapunov stable control methodology that permits the nonlinearly damped pendulum system to start from any given initial conditions and reach a desired final state. It is assumed that the multi-body system—called the 'nominal system'—is precisely known. Based on a suitable Lyapunov function, a nonlinear controller is obtained in closed form that simultaneously minimizes a user-specified norm of the control effort [6]. The method is inspired by results in analytical dynamics and is much simpler than those inspired by LQ methods such as SDRE [7], Sontag's formula method, and related CLF-based methods [8–10]. It has an advantage over the standard backstepping method [10,11] in that it not only yields a Lyapunov stable control but also minimizes a control cost at each instant of time while using a user-desired Lyapunov function for the *entire* system. Åström [12] considers the swing-up of a one-mass pendulum using energy considerations providing a novel physically based approach to its control. Aguilar-Ibáñez and Azuela [13] have worked on stabilizing the underactuated Furuta pendulum, and they obtain local asymptotic stability around the vertical position of the pendulum using a suitable Lyapunov function in combination with partial feedback linearization. More recently, Aguilar-Ibáñez et al. [14] have considered the underactuated control of an inverted (planar) pendulum mounted on a cart that moves along a straight line. They develop an observer-based controller that makes the time derivative of the energy semi-negative definite and thereafter use Lasalle's Theorem for the closed-loop stability analysis. A quite different approach that is inspired by analytical dynamics has been taken to the control of mechanical systems in Refs. [15–18]. The control objectives are cast in the form of nonholonomic constraints that are enforced using the fundamental equation of motion obtained from analytical dynamic [18,19]. Successful applications of this approach for various complex nonlinear mechanical systems can be found in Refs. [19,20].

In contrast to the methods used in Refs. [12–14], it is this control approach that is developed and used in this paper. It does not use conventional methods of control design and comes from recent developments of the theory of constrained motion of mechanical systems. A user-defined Lyapunov function and a user-specified rate of its decay are used as constraints on the mechanical system, and the equations of motion of the constrained (controlled) system are directly obtained using the fundamental equation of mechanics (see Refs. [6,15–17]). Exact closed-form expressions for the (generalized) control force are obtained without making any assumptions/linearizations on the nonlinear system and without imposing any a priori structure on the controller. An important characteristic of the nonlinear controller so obtained is that it is optimal in the sense that it simultaneously minimizes a user-defined quadratic control cost at *each* instant of time. Various Lyapunov functions can be used; proper choices of the Lyapunov function render the control globally asymptotically stable [6]. Simulation results in which a user-specified quadratic control cost is minimized and a 10-body pendulum is held stable in various so-called unstable equilibrium positions such as the 'inverted pendulum' position are demonstrated. For example, closed-form globally stable (optimal) control required for the 10-body pendulum system to: (i) swing-up from its stable static equilibrium position, (ii) then take a full circle past its vertically inverted position, and (iii) come all the way around to finally stand stably in the vertically inverted position, is obtained with considerable simplicity and ease (see Fig. 3). The current literature (see Refs. [12–14]) has been limited to the validation of control methods for much simpler types of motion control such as the swing-up of a pendulum system from its static, stable, equilibrium position directly to its vertically inverted position. In fact, such studies have been reported for pendulum systems made up of just two or three bodies.

It is important to note that the pendulum system described (and controlled) in this paper is composed of

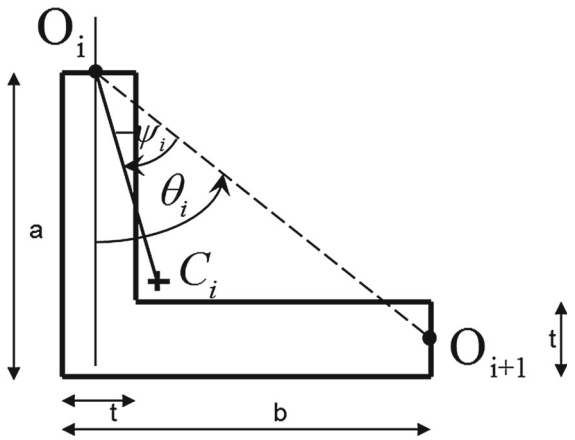

Fig. 2 Geometry of the L-shaped body that forms the ith body in the 10-body pendulum. The hinges are located at O_i and O_{i+1}. For $a = 0.4$ m, $b = 0.5$ m and $t = 0.1$ m, the angle $\theta_i \approx 52.125^o$ and the angle ψ_i shown in the figure is about 24.444^o

individual bodies whose mass centers do not lie along the line passing through their respective hinges (see Figs. 1, 2). Besides being a better approximation of reality, when such a pendulum system is being swung-up to an 'inverted' position, considerably larger destabilizing gravity-induced torques about the base pivot O of the pendulum can be induced than when the center of mass of each individual body is restricted to lie along the line passing through its hinges. In addition, the use of a 10-body pendulum system further increases this instability induced by these torques, thereby making the control problem addressed herein substantially more challenging.

The third part of this paper deals with the question of controlling an actual physical n-body pendulum whose description is not precisely known. From a practical standpoint, this is the situation that is most commonly encountered in dynamical systems with even a moderate degree of complexity. In what follows, our best estimate (often an educated guess) of the description of the actual system at hand will be referred to as the 'nominal system.' Thus, the nominal system comprises our best assessment of the description of the actual physical system, and therefore, the description that it provides of the actual system is correct only to within some uncertainty bounds. One would then want to control the actual physical system whose description is not exactly known, so that it meets the dynamical expectations imposed on the nominal system, which in fact is the only system whose description one has in hand. This is done through the development of a simple additional continuous controller, which is based on the concept of a generalized sliding surface, that tracks to within pre-specified error bounds (that can be made as small as desired) the motion of the nominal system in the presence of norm-bounded uncertainties in our knowledge of the actual system. To preserve the thread of thought, proofs related to the development of this continuous controller are given in Appendix. In Sect. 4, a brief review of the literature on the control of uncertain system is provided.

Closed-form controllers that stabilize a 10-body nonlinearly damped pendulum system in the various unstable equilibrium positions that were used earlier with the nominal system are now obtained for the actual system and their effectiveness is shown. Thus, the efficacy of the control methodology and the simplicity of its implementation for the nominal system and for the

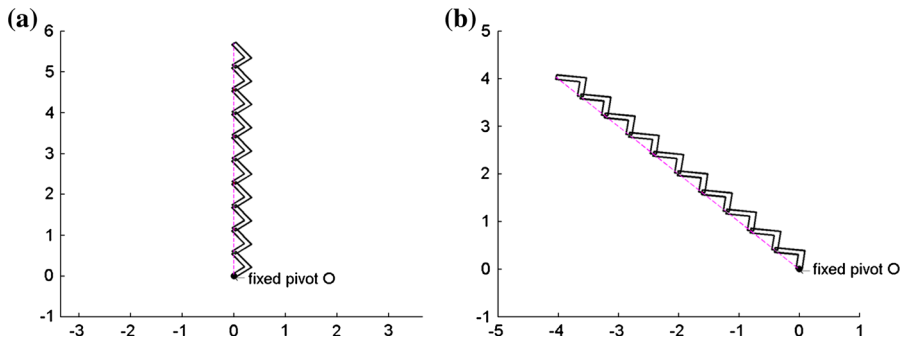

Fig. 3 **a** Final configuration of the 10-body pendulum system in Cases (i) and (iii) in which the system is required to come to rest in the upside-down 'inverted' position. **b** Final configuration of the system in Case (ii) in which the pendulum system is required to come to rest so that $\theta_i^{final} = 5\pi/4, \forall i$

actual system, whose description may be uncertain, are demonstrated.

2 Derivation of the general equations of motion of an n-body pendulum

Consider the n-body pendulum that undergoes planar motions suspended from the point O (see Fig. 1). The ith body in the pendulum has mass m_i, and its moment of inertia about its center of mass (CM), which is located at C_i, is J_i. The coordinates of the point C_i in the inertial coordinate frame OXY are (x_i, y_i). The distance between the upper and the lower hinges in the ith body is l_i, and the distance from the upper hinge to its CM is $b_i l_i$. The line joining the two hinges in the ith body makes an angle θ_i with the vertical, measured in the counterclockwise direction (see Fig. 1). Similarly, the angle made by the line joining the upper hinge to the CM of the ith body makes an angle ψ_i with the line joining the two hinges; as shown in the figure, this angle is again measured counterclockwise from the line joining the two hinges.

For purposes of uniformity in our formulation of the equations of motion, we have used two hinges within each body. When viewed in the stable static equilibrium position of the n-body pendulum, the upper hinge in each body is the location, where it is connected to the body immediately above, and the lower hinge, where it is connected to the body immediately below. However, since the nth body has nothing below it, we can locate an imaginary 'lower hinge' (shown by the square in Fig. 1) at any point in it. Specifically for convenience, were this imaginary lower hinge placed at the CM of this nth body, then we would have $\psi_n = 0$; if, further, b_n were set to unity, then the distance from the CM of the nth body to its upper hinge, which is given by $b_n l_n$, would then simply be l_n.

A similar situation arises when the pendulum system comprises of just a single body suspended from the point O. An imaginary 'second hinge' can be placed at any location in this body other than at O, say at the point O_1 as shown in the figure. The line OO_1 joining the two hinges is shown by a dashed line. The purpose of this second hinge is simply to provide a direction so that the angle θ_1 can be measured in the counterclockwise direction from the vertical. Using elementary Newtonian mechanics and taking moments about the fixed origin O, we get the equation of motion for this one-body pendulum as

$$\left[J_1 + m_1(b_1 l_1)^2\right]\ddot{\theta}_1 + m_1 g(b_1 l_1)\sin(\theta_1 + \psi_1) = 0. \tag{1}$$

Alternatively, as discussed before, the point O_1 could have been chosen to coincide with the location C_1 of the CM of the body so that $\psi_1 = 0$. Now θ_1 is the angle made by the line OC_1 with the vertical. If, further, one sets $b_1 = 1$, then l_1 can now be interpreted as simply the distance of the CM of the body from the hinge at O. Setting $b_1 = 1$ and $\psi_1 = 0$ in Eq. (1), we get the equation of motion of the pendulum in its standard form, namely

$$\left[J_1 + m_1 l_1^2\right]\ddot{\theta}_1 + m_1 g l_1 \sin\theta_1 = 0. \tag{2}$$

where l_1 is now the distance of the CM of the body from O. Though a trivial result, it is required in the proof of our general result where we will be interested in obtaining the equations of motion of a planar n-body pendulum, with $n > 1$.

The algebraic complexity of the derivation of the Lagrange equations of motion increases greatly as the number of bodies in the system increase, and here, we use a new and novel approach that utilizes mathematical induction on the number of bodies (degrees of freedom) of the system. We begin by stating our result.

Result: The Lagrange equations of motion of the undamped n-body pendulum described above (see Fig. 1) are given by

$$M^{(n)}(\theta^{(n)})\,\ddot{\theta}^{(n)} + S^{(n)}(\theta^{(n)})\left[\dot{\theta}^{(n)}\right]^2 + F^{(n)}(\theta^{(n)}) = 0, \tag{3}$$

where the n-vector (n by 1 vector) $\theta^{(n)} = [\theta_1, \theta_2, \ldots, \theta_n]^T$, and the n-vector $\left[\dot{\theta}^{(n)}\right]^2 := [\dot{\theta}_1^2, \dot{\theta}_n^2, \ldots, \dot{\theta}_n^2]^T$. The superscripts '$(n)$' in Eq. (3) explicitly point out that the equations are for an n-body pendulum; the matrices $M^{(n)}$ and $S^{(n)}$ are therefore n by n matrices, and the vector $F^{(n)}$ is an n by 1 column vector (n-vector). The elements, $m_{i,j}^{(n)}$, of the symmetric matrix $M^{(n)}$ are explicitly given by the relations

$$m_{i,i}^{(n)} = J_i + l_i^2\{m_i b_i^2 + \bar{m}_i\}, \quad 1 \le i \le n, \tag{4}$$

and,

$$m_{i,j}^{(n)} = l_i l_j[m_j b_j \cos(\theta_{ij} - \psi_j) + \bar{m}_j \cos(\theta_{ij})], \quad 1 \le i < j \le n, \tag{5}$$

where we define

$$\theta_{ij} = \theta_i - \theta_j, \bar{m}_i = \sum_{k=i+1}^{n} m_k, \text{ and } \bar{m}_n = 0. \tag{6}$$

The elements, $s_{i,j}^{(n)}$, of the skew-symmetric matrix $S^{(n)}$, whose diagonal elements are of course all zero, are given by the relations

$$s_{i,j}^{(n)} = l_i l_j [m_j b_j \sin(\theta_{ij} - \psi_j) + \bar{m}_j \sin(\theta_{ij})], \quad 1 \le i < j \le n, \tag{7}$$

and the elements, $f_i^{(n)}$, of the n-vector $F^{(n)}$ are given by the relations

$$f_i^{(n)} = g l_i \{m_i b_i \sin(\theta_i + \psi_i) + \bar{m}_i \sin(\theta_i)\}, \quad 1 \le i \le n. \tag{8}$$

Proof We note, using Eqs. (4) and (8), that the result is trivially true for $n = 1$ as seen from Eq. (1). To proceed with our proof by induction, we assume that Eqs. (3)–(8) are true for any $n = N \ge 1$, i.e., for an N-body pendulum. We then need to prove that they are true for $n = N + 1$, i.e., for an $(N + 1)$-body pendulum.

A comparison of elements of the symmetric matrices $M^{(N)}$ and $M^{(N+1)}$ using Eqs. (4) and (5) reveals that if these equations are correct for $N \ge 1$, then

$$\begin{aligned}
&m_{i,j}^{(N+1)} - m_{i,j}^{(N)} = m_{j,i}^{(N+1)} - m_{j,i}^{(N)} := \Delta m_{i,j} \\
&\quad = m_{N+1} l_i l_j \cos(\theta_{ij}), \\
&\quad 1 \le i, j \le N, \\
&m_{i,N+1}^{(N+1)} = m_{N+1,i}^{(N+1)} \\
&\quad = m_{N+1} l_i b_{N+1} l_{N+1} \cos(\theta_{iN+1} - \psi_{N+1}), \\
&\quad 1 \le i \le N, \\
&m_{N+1,N+1}^{(N+1)} = J_{N+1} + m_{N+1} l_{N+1}^2 b_{N+1}^2.
\end{aligned} \tag{9}$$

Similarly, a comparison of the elements of the skew-symmetric matrices $S^{(N)}$ and $S^{(N+1)}$ using Eq. (7) shows that if this relation is correct then

$$\begin{aligned}
&s_{i,j}^{(N+1)} - s_{i,j}^{(N)} := \Delta s_{i,j} \\
&\quad = m_{N+1} l_i l_j \sin(\theta_{ij}), \ 1 \le i, j \le N, \\
&s_{i,N+1}^{(N+1)} = -s_{N+1,i}^{(N+1)} \\
&\quad = m_{N+1} l_i l_{N+1} b_{N+1} \sin(\theta_{iN+1} - \psi_{N+1}), \\
&\quad 1 \le i \le N.
\end{aligned} \tag{10}$$

Lastly, a comparison of Eq. (8) for the vectors $F^{(N)}$ and $F^{(N+1)}$ shows that, if correct, then we must have

$$\begin{aligned}
&f_i^{(N+1)} - f_i^{(N)} := \Delta f_i = m_{N+1} g l_i \sin\theta_i, \ 1 \le i \le N, \\
&f_{N+1}^{(N+1)} = m_{N+1} g b_{N+1} l_{N+1} \sin(\theta_{N+1} + \psi_{N+1}).
\end{aligned} \tag{11}$$

Hence, we are required to show that in going from an N-body pendulum to an $(N+1)$-body pendulum $(N \ge 1)$, the changes in the matrices M and S and in the vector F must be as prescribed by relations (9)–(11). Showing this would then complete our proof.

But the difference between the N-body pendulum and the $(N + 1)$-body pendulum is just the addition of the $(N+1)$th body! And hence all the terms on the right-hand side of relations (9), (10), and (11) must come *solely* from the Lagrangian L of only the $(N + 1)$th body. Since the coordinates (x_{N+1}, y_{N+1}) of the CM of the $(N + 1)$th body are (for $N \ge 1$),

$$\begin{aligned}
x_{N+1} &= \sum_{j=1}^{N} l_j \sin\theta_j + b_{N+1} l_{N+1} \sin(\theta_{N+1} + \psi_{N+1}), \\
y_{N+1} &= -\sum_{j=1}^{N} l_j \cos\theta_j - b_{N+1} l_{N+1} \cos(\theta_{N+1} + \psi_{N+1}),
\end{aligned} \tag{12}$$

its Lagrangian L is

$$\begin{aligned}
L := T - V &= \frac{1}{2} m_{N+1} (\dot{x}_{N+1}^2 + \dot{y}_{N+1}^2) \\
&\quad + \frac{1}{2} J_{N+1} \dot{\theta}_{N+1}^2 - m_{N+1} g y_{N+1},
\end{aligned} \tag{13}$$

where T denotes the kinetic energy of the (N+1)th body and V denotes its gravitational potential energy.

Our aim is to find how this Lagrangian L, through its inclusion, alters the Lagrange equations of motion of the N-body pendulum, thereby providing us with the Lagrange equations for the $(N + 1)$-body pendulum.

We denote the Lagrange operator $\mathcal{L}_i(*) = \frac{d}{dt}\left(\frac{\partial *}{\partial \dot{\theta}_i}\right) - \left(\frac{\partial *}{\partial \theta_i}\right)$. Then, from relation (12), we obtain

$$\begin{aligned}
\mathcal{L}_i(L) &= m_{N+1}\left[\frac{d}{dt}\left(\frac{\partial \dot{x}_{N+1}}{\partial \dot{\theta}_i}\dot{x}_{N+1}\right) - \frac{\partial \dot{x}_{N+1}}{\partial \theta_i}\dot{x}_{N+1}\right] \\
&\quad + m_{N+1}\left[\frac{d}{dt}\left(\frac{\partial \dot{y}_{N+1}}{\partial \dot{\theta}_i}\dot{y}_{N+1}\right) - \frac{\partial \dot{y}_{N+1}}{\partial \theta_i}\dot{y}_{N+1}\right] \\
&\quad + \delta_{i,N+1} J_{N+1}\ddot{\theta}_{N+1} + \frac{\partial V}{\partial \theta_i} \\
&= m_{N+1}\left[\frac{d}{dt}\left(\frac{\partial x_{N+1}}{\partial \theta_i}\dot{x}_{N+1}\right) - \frac{\partial \dot{x}_{N+1}}{\partial \theta_i}\dot{x}_{N+1}\right] \\
&\quad + m_{N+1}\left[\frac{d}{dt}\left(\frac{\partial y_{N+1}}{\partial \theta_i}\dot{y}_{N+1}\right) - \frac{\partial \dot{y}_{N+1}}{\partial \theta_i}\dot{y}_{N+1}\right] \\
&\quad + \delta_{i,N+1} J_{N+1}\ddot{\theta}_{N+1} + \frac{\partial V}{\partial \theta_i} \\
&= m_{N+1}\frac{\partial x_{N+1}}{\partial \theta_i}\ddot{x}_{N+1} + m_{N+1}\frac{\partial y_{N+1}}{\partial \theta_i}\ddot{y}_{N+1} \\
&\quad + \delta_{i,N+1} J_{N+1}\ddot{\theta}_{N+1} + \frac{\partial V}{\partial \theta_i}
\end{aligned} \tag{14}$$

where $\delta_{i,N+1}$ is the Kronecker delta. In the second and third equalities above, we have used the relations $\frac{\partial \dot{x}_{N+1}}{\partial \dot{\theta}_i} = \frac{\partial x_{N+1}}{\partial \theta_i}$ and $\frac{d}{dt}\left(\frac{\partial x_{N+1}}{\partial \theta_i}\right) = \frac{\partial \dot{x}_{N+1}}{\partial \theta_i}$, and similar relations for y_{N+1}. Using relation (12), we then have

$$\begin{aligned}\ddot{x}_{N+1} = &\sum_{j=1}^{N}\left[l_j\cos\theta_j\ddot{\theta}_j - l_j\sin\theta_j\dot{\theta}_j^2\right]\\ &+ b_{N+1}l_{N+1}\Big[\cos(\theta_{N+1}+\psi_{N+1})\ddot{\theta}_{N+1}\\ &- \sin(\theta_{N+1}+\psi_{N+1})\dot{\theta}_{N+1}^2\Big] \qquad (15)\end{aligned}$$

and similarly,

$$\begin{aligned}\ddot{y}_{N+1} = &\sum_{j=1}^{N}\left[l_j\sin\theta_j\ddot{\theta}_j + l_j\cos\theta_j\dot{\theta}_j^2\right]\\ &+ b_{N+1}l_{N+1}\Big[\sin(\theta_{N+1}+\psi_{N+1})\ddot{\theta}_{N+1}\\ &+ \cos(\theta_{N+1}+\psi_{N+1})\dot{\theta}_{N+1}^2\Big]. \qquad (16)\end{aligned}$$

Using relations (12), (15), and (16) in Eq. (14) gives $\mathcal{L}_i$ for $1 \le i \le N$, and we get

$$\begin{aligned}\mathcal{L}_i(L) = &\, m_{N+1}l_ib_{N+1}l_{N+1}\Big[\cos(\theta_i)\cos(\theta_{N+1}\\ &+\psi_{N+1})\ddot{\theta}_{N+1} - \cos(\theta_i)\sin(\theta_{N+1}\\ &+\psi_{N+1})\dot{\theta}_{N+1}^2\Big]\\ &+ m_{N+1}l_i\cos(\theta_i)\sum_{j=0}^{N}\Big[l_j\cos(\theta_j)\ddot{\theta}_j\\ &- l_j\sin(\theta_j)\dot{\theta}_j^2\Big] + m_{N+1}l_i\sin(\theta_i)\\ &\times\sum_{j=0}^{N}\Big[l_j\sin(\theta_j)\ddot{\theta}_j + l_j\cos(\theta_j)\dot{\theta}_j^2\Big]\\ &+ m_{N+1}l_ib_{N+1}l_{N+1}\Big[\sin(\theta_i)\\ &\times\sin(\theta_{N+1}+\psi_{N+1})\ddot{\theta}_{N+1}\\ &+\sin(\theta_i)\cos(\theta_{N+1}+\psi_{N+1})\dot{\theta}_{N+1}^2\Big] + \frac{\partial V}{\partial\theta_i},\\ &\qquad (17)\end{aligned}$$

which simplifies to

$$\begin{aligned}\mathcal{L}_i(L) = &\sum_{j=1}^{N}\underbrace{m_{N+1}l_il_j\cos(\theta_i-\theta_j)}_{\Delta m_{i,j}}\ddot{\theta}_j\\ &+\underbrace{m_{N+1}l_ib_{N+1}l_{N+1}\cos(\theta_i-\theta_{N+1}-\psi_{N+1})}_{m_{i,N+1}^{(N+1)}}\ddot{\theta}_{N+1}\\ &+\sum_{j=1}^{N}\underbrace{m_{N+1}l_il_j\sin(\theta_i-\theta_j)}_{\Delta s_{i,j}}\dot{\theta}_j^2\\ &+\underbrace{m_{N+1}l_ib_{N+1}l_{N+1}\sin(\theta_i-\theta_{N+1}-\psi_{N+1})}_{s_{i,N+1}^{(N+1)}}\dot{\theta}_{N+1}^2\\ &+\underbrace{m_{N+1}gl_i\sin\theta_i}_{\Delta f_i},\ 1\le i\le N. \qquad (18)\end{aligned}$$

This equation identifies the terms that need to be added to the (i, j) elements of the matrices $M^{(N)}$ and $S^{(N)}$ to obtain the corresponding (i, j) elements of the matrices $M^{(N+1)}$ and $S^{(N+1)}$ for $1 \le i \le N$ and $1 \le j \le N+1$. They are the same as those shown in Eqs. (9) and (10). Also, the elements Δf_i shown in Eq. (18) need to be added to the N elements of the N-vector $F^{(N)}$ to obtain the corresponding (first) N elements of the vector $F^{(N+1)}$; they too are the same as those given in relation (11). The third term on the right-hand side of Eq. (18) shows that the upper left N by N submatrix of $S^{(N+1)}$ is skew symmetric; this is because the N by N matrix $S^{(N)}$ is assumed to be skew symmetric and we are adding to this N by N matrix another skew-symmetric matrix $\Delta s_{i,j}$. In a similar manner we compute the additional Lagrange equation that results when we go from an N-body pendulum to an $(N+1)$-body pendulum ($N \ge 1$). We have for

$$\begin{aligned}\mathcal{L}_{N+1}(L) = &\, m_{N+1}b_{N+1}l_{N+1}\cos(\theta_{N+1}+\psi_{N+1})\\ &\times\sum_{i=1}^{N}\Big[l_i\cos(\theta_i)\ddot{\theta}_i - l_i\sin(\theta_i)\theta_i^2\Big]\\ &+m_{N+1}b_{N+1}^2l_{N+1}^2[\cos^2(\theta_{N+1}+\psi_{N+1})\ddot{\theta}_{N+1}\\ &-\cos(\theta_{N+1}+\psi_{N+1})\sin(\theta_{N+1}+\psi_{N+1})\dot{\theta}_{N+1}^2]\\ &+m_{N+1}b_{N+1}l_{N+1}\sin(\theta_{N+1}+\psi_{N+1})\\ &\times\sum_{i=1}^{N}\Big[l_i\sin(\theta_i)\ddot{\theta}_i + l_j\cos(\theta_i)\theta_i^2\Big]\\ &+J_{N+1}\ddot{\theta}_{N+1} + \frac{\partial V}{\partial\theta_{N+1}}\\ &+m_{N+1}b_{N+1}^2l_{N+1}^2[\sin^2(\theta_{N+1}+\psi_{N+1})\ddot{\theta}_{N+1}\\ &+\cos(\theta_{N+1}+\psi_{N+1})_i\sin(\theta_{N+1}+\psi_{N+1})\dot{\theta}_{N+1}^2],\\ &\qquad (19)\end{aligned}$$

which simplifies to

$$\begin{aligned}
&\mathcal{L}_{N+1}(L)\\
&= \sum_{i=1}^{N} \underbrace{m_{N+1} b_{N+1} l_{N+1} l_j \cos(\theta_i - \theta_{N+1} - \psi_{N+1})}_{m^{(N+1)}_{N+1,\,i}} \ddot{\theta}_i\\
&\quad + \sum_{i=1}^{N} \underbrace{-m_{N+1} b_{N+1} l_{N+1} l_i \sin(\theta_i - \theta_{N+1} - \psi_{N+1})}_{s^{(N+1)}_{N+1,\,i}} \dot{\theta}_i^2\\
&\quad + \underbrace{(m_{N+1} b_{N+1}^2 l_{N+1}^2 + J_{N+1})}_{m^{(N+1)}_{N+1,\,N+1}} \ddot{\theta}_{N+1}\\
&\quad + \underbrace{m_{N+1} l_{N+1} g \sin(\theta_{N+1} + \psi_{N+1})}_{f^{(N+1)}_{N+1}}, \qquad (20)
\end{aligned}$$

On the right-hand side of Eq. (20), terms related to the elements of the last row of the matrices $M^{(N+1)}$ and $S^{(N+1)}$ are identified, which are the same as those given in relations (9) and (10). We note from relations (18) and (20) that $s^{(N+1)}_{N+1,\,i} = -s^{(N+1)}_{i,\,N+1}$, $1 \le i \le N+1$, and therefore, the matrix $S^{(N+1)}$ is skew symmetric. Also, the $(N+1)$st element of the vector $F^{(N+1)}$ is given by $f^{(N+1)}_{N+1}$, as required from relation (11). We observe from relations (18) and (20) that the mass matrix $M^{(N+1)}$ is symmetric, yet one does not need to prove this. Since the coordinates of the center of mass (x_i, y_i) of the ith body, $1 \le i \le N+1$, when expressed in the θ coordinates do not contain time explicitly, Lagrangian mechanics guarantees that the matrix is symmetric! □

Remark 1 For the n-th body (and only for the nth body) of the n-body pendulum, we can set $\psi_n = 0$, and as discussed before, also set $b_n = 1$ so that l_n is now the distance of the CM of the nth body to the hinge in it. The other l_i's, $1 \le i \le n-1$, of course retain their usual meanings. The angle θ_n (and only θ_n, none of the other θ_i's) now denotes the angle (measured counterclockwise) that the line joining the hinge in the nth body to its CM makes with the vertical (see Fig. 1).

Then, from Eqs. (4)–(6), the elements $m^{(n)}_{i,j}$ of the symmetric matrix $M^{(n)}$ in Eq. (3) are explicitly given by

$$\begin{aligned}
m^{(n)}_{i,\,i} &= J_i + l_i^2\{m_i b_i^2\\
&\quad + \bar{m}_i\}, \quad 1 \le i \le n-1;\\
m^{(n)}_{i,j} &= l_i l_j [m_j b_j \cos(\theta_{ij} - \psi_j)\\
&\quad + \bar{m}_j \cos\theta_{ij}], \quad 1 \le i < j \le n-1;\\
m^{(n)}_{i,n} &= l_i l_n m_n \cos\theta_{in}, \quad 1 \le i \le n-1;\\
m^{(n)}_{n,\,n} &= J_n + m_n l_n^2, \qquad (21)
\end{aligned}$$

where, as before, $\bar{m}_i = \sum_{k=i+1}^{n} m_k$ with $\bar{m}_n = 0$.

Similarly, from Eq. (7), the elements $s^{(n)}_{i,j}$ of the skew-symmetric matrix $S^{(n)}$ in Eq. (3) can be explicitly written as

$$\begin{aligned}
s^{(n)}_{i,j} &= l_i l_j [m_j b_j \sin(\theta_{ij} - \psi_j)\\
&\quad + \bar{m}_j \sin(\theta_{ij})], \ 1 \le i < j \le n-1,\\
s^{(n)}_{i,\,n} &= m_n l_i l_n \sin\theta_{in}, \ 1 \le i \le n-1. \qquad (22)
\end{aligned}$$

and the elements $f^{(n)}_i$ of the column vector $F^{(n)}$ can be written as

$$\begin{aligned}
f^{(n)}_i &= g l_i \{m_i b_i \sin(\theta_i + \psi_i)\\
&\quad + \bar{m}_i \sin(\theta_i)\}, \ 1 \le i \le n-1,\\
f^{(n)}_n &= m_n g l_n \sin\theta_n \qquad (23)
\end{aligned}$$

□

Remark 2 If the n-body pendulum is made up of all 'straight' links/bodies, as has nearly always been assumed in the research literature hereto, then the center of mass of each body will lie on the line joining its hinges; hence, $\psi_i = 0, 1 \le i \le n$. The equation of motion (3) then simplifies further since in the relations given in Eqs. (4)–(8) and Eqs. (21)–(23) for the elements of $M^{(n)}$, $S^{(n)}$, and $F^{(n)}$, we set $\psi_i = 0, 1 \le i \le n$.

Remark 3 Consider a damped n-body planar pendulum in which the hinges provide dissipative torques. Assume that the torque generated at the ith hinge (the first hinge is at O, the second at O_1, etc., see Fig. 1) is expressed as

$$\begin{aligned}
&\hat{c}_i(\dot{\theta}_i - \dot{\theta}_{i-1}) + \hat{\mathrm{d}}_i(\dot{\theta}_i - \dot{\theta}_{i-1})^3, \ 1 \le i \le n,\\
&\quad \text{with } \dot{\theta}_0 := 0, \qquad (24)
\end{aligned}$$

where the $\hat{c}_i, \hat{d}_i, i = 1, \ldots, n$, are positive constants. The above relation thus assumes 'linear plus cubic' damping. Then, the equation of motion of this damped n-body pendulum is given by

$$\begin{aligned}
&M^{(n)}(\theta^{(n)})\,\ddot{\theta}^{(n)} + S^{(n)}(\theta^{(n)})\left[\dot{\theta}^{(n)}\right]^2 + C^{(n)}\dot{\theta}^{(n)}\\
&\quad + D^{(n)}(\dot{\theta}^{(n)}) + F^{(n)}(\theta^{(n)}) = 0 \qquad (25)
\end{aligned}$$

where the n-vector $\dot{\theta}^{(n)} := d\theta^{(n)}/dt$. The the elements $c^{(n)}_{i,j}$ of the n by n constant, symmetric, tridiagonal

matrix $C^{(n)}$ are obtained by using the virtual work done by the dissipative torques as

$$c_{i,i}^{(n)} = \hat{c}_i + \hat{c}_{i+1}, \qquad 1 \le i \le n,$$
$$c_{i,i+1}^{(n)} = c_{i+1,i}^{(n)} = -\hat{c}_{i+1}, \quad 1 \le i \le n-1 \tag{26}$$

where we define $\hat{c}_{n+1} := 0$. Similarly, using virtual work, the n-vector $D^{(n)}$ has elements $d_i^{(n)}$ given by

$$d_i^{(n)} = \hat{d}_i(\dot{\theta}_i - \dot{\theta}_{i-1})^3 - \hat{d}_{i+1}(\dot{\theta}_{i+1} - \dot{\theta}_i)^3, 1 \le i \le n \tag{27}$$

where we again define $\dot{\theta}_0 = \hat{d}_{n+1} = 0$.

The term $C^{(n)}\dot{\theta}^{(n)}$ in Eq. (25) gives rise to linear damping in the system, and the vector $D^{(n)}(\dot{\theta}^{(n)})$ gives rise to nonlinear cubic damping. Other damping models can be similarly incorporated using the n-vector $D^{(n)}$ in Eq. (25).

3 Control of an n-body damped planar pendulum

3.1 Explicit control of n-body pendulum

Our aim in this section to is obtain an explicit closed-form control of the n-body pendulum described in the previous section that simultaneously minimizes a user-specified quadratic control cost. It is assumed that the parameters that describe the pendulum system are precisely known and that the description of the system is therefore accurate. From a practical standpoint though, such precision might not be possible in the modeling of even moderately complex mechanical systems. This issue will be dealt with in the next section, where uncertainties in the description of the pendulum system will be considered. For the present, we assume that the system's description is precisely available.

We would prefer the control to be Lyapunov asymptotically stable, and global, so that we can control the nonlinear system from any given initial state $(\theta^{initial}, \dot{\theta}^{initial})$ to any final state $(\theta^{final}, \dot{\theta}^{final})$. To do this, we use the fundamental equation of mechanics (see Refs.[6,15–17]).

The n-body pendulum system is highly nonlinear. Assuming further that it is also nonlinearly damped as in Remark 3, the equation of motion of the controlled system is given by (we now omit the superscript '(n)' for clarity)

$$M(\theta)\,\ddot{\theta} + S(\theta)\left[\dot{\theta}\right]^2 + C\dot{\theta} + D(\dot{\theta}) + F(\theta) = Q^C(\theta, \dot{\theta}) \tag{28}$$

where θ is now an n-vector, and Q^C is the generalized control force n-vector that needs to be determined. Equation (28) can be rewritten for further notational convenience as

$$M\ddot{\theta} = -\{S\left[\dot{\theta}\right]^2 + C\dot{\theta} + D + F\} + Q^C := Q + Q^C \tag{29}$$

where we have suppressed the arguments of the various quantities.

We begin by choosing a suitable Lyapunov function V that is positive definite with $V(\theta^{final}, \dot{\theta}^{final}) = 0$ and is positive everywhere else and, utilizing the result in Ref. [6], enforce the constraint on the controlled system so that its trajectory always satisfies the relation

$$\frac{dV(\theta, \dot{\theta})}{dt} = -\alpha V(\theta, \dot{\theta}), \tag{30}$$

where $\alpha > 0$ is a suitable constant. From Lyapunov's second method, we know that if the equality (30) is satisfied, the system will have an asymptotically stable equilibrium point at $(\theta^{final}, \dot{\theta}^{final})$ [10]. Furthermore, if the choice of our Lyapunov function is such that it is radially unbounded, then we are assured global asymptotic stability. Our control methodology is based on enforcing Eq. (30) as a nonholonomic constraint on the mechanical system. Note that our methodology consists of exactly specifying the rate at which the Lyapunov function decays which is different from the control methods available in the literature for general dynamical systems that only ensure that the rate of change of Lyapunov function is negative at each instant of time [8–11].

Equation (30) can be written as

$$A(\theta, \dot{\theta})\ddot{\theta} = b(\theta, \dot{\theta}) \tag{31}$$

where the row n-vector A and the scalar b are, respectively, given by

$$A = \frac{\partial V}{\partial \dot{\theta}}, \text{ and } b = -\frac{\partial V}{\partial \theta}\dot{\theta} - \alpha V. \tag{32}$$

The explicit generalized control force that enforces the constraint Eq. (31) while simultaneously minimizing the control cost

$$J(t) = [Q^C]^T N(\theta) Q^C \tag{33}$$

for a given positive definite weighting matrix $N(\theta)$ is obtained, using the fundamental equation of mechanics [6], as

$$Q^C = N^{-1/2} G^+ (b - AM^{-1}Q) \tag{34}$$

where the matrix $G = A(N^{1/2}M)^{-1}$ and G^+ denotes the Moore–Penrose inverse of the matrix G. It is important that the function V and the parameter α be chosen so that the constraint given by Eq. (31) is consistent at all times. As mentioned before, if V is radially unbounded, the equilibrium point $(\theta^{final}, \dot{\theta}^{final})$ is globally asymptotically stable. In the following subsection, we provide a numerical example.

3.2 Numerical example

We consider a 10-body damped, planar pendulum in which all the bodies are identical and each body is L-shaped. Figure 2 shows the geometry of the ith body. The dimensions of the outer edges of the arms of each L-shaped body are taken to be a and b, and the width, t. See Fig. 2. We assume that all the bodies are of uniform (and constant) thickness t_h perpendicular to the paper and that the density of the material of each body is ρ.

For simplicity, the Lyapunov function V is chosen to be

$$V = \frac{1}{2}a_1(\theta - \theta^{final})^T(\theta - \theta^{final}) + \frac{1}{2}a_2\dot{\theta}^T\dot{\theta} + a_{12}\dot{\theta}^T\theta \tag{35}$$

so that the equilibrium point is $(\theta^{final}, 0)$. To ensure that V is positive definite, we require that $a_1 > 0$, $a_1a_2 > a_{12}^2$.

The parameter α in Eq. (30) is chosen to be equal to $2a_{12}/a_2$ to ensure consistency of this equation (see Ref. [6] and the Appendix of Ref. [29]), and the weighting matrix N in Eq. (32) is set to M^{-1}. With this weighing matrix, noting that A is a row vector, relation (34) simply becomes

$$Q^C = \frac{A^T}{(AM^{-1}A^T)}(b - AM^{-1}Q) \quad . \tag{36}$$

Equation (36) explicitly gives the control torque that is required to be applied to each hinge of the pendulum system. We note in passing that this would be the constraint torque that nature would apply to the pendulum system were it required to satisfy the constraint given in Eq. (31); it is the constraint torque given directly by the fundamental equation of motion in analytical dynamics [15–17].

For the simulations shown below, the following parameter values are used for the geometry of each of the L-shaped bodies: $a = 0.4$ m, $b = 0.5$ m, $t = 0.1$ m (see Fig. 2). The mass of each body is then $0.08t_h\rho$, and its moment of inertia about its center of mass is $0.002833t_h\rho$. For numerical computations, we take $t_h = 0.01$ m, and $\rho = 7850$ kg/m^3. Thus, each body has a mass of 6.28 kg. The parameters describing the nonlinear damping (see in Remark 3 of Sect. 2) are chosen to be $\hat{c}_i = 0.01$ N-m-s/rad, $i = 1, \ldots, n$, and $\hat{d}_i = 0.001$ N-m-s^3/rad^3, $i = 1, \ldots, n$. These parameters describe the pendulum system, and in this section, it is assumed that they are precisely known. (In the following section, the masses of all the bodies will be taken to be uncertain, assuming measurement errors in their determination.)

The parameters used to describe the Lyapunov function in Eq. (34) are $a_1 = 1, a_2 = 1, a_{12} = 0.5$ so that $\alpha = 1$ in Eq. (30). Three different simulations are presented. Each simulation starts from the stable static equilibrium position, and in each simulation, the 10-body damped pendulum is "swung-up" from rest. The following three cases are shown:

(i) The system is swung-up and is required to come to rest upside down in the 'inverted pendulum' position with all its hinges aligned vertically above the fixed pivot O (see Fig. 3a) so that $\theta_i^{final} = \pi, \dot{\theta}_i^{final} = 0, \forall i$;

(ii) the system is swung-up and is required to come to rest past its inverted 'upside-down' position so that all the hinges lie along the line $x + y = 0$ in the second quadrant in the XY plane with $\theta_i^{final} = 5\pi/4, \dot{\theta}_i^{final} = 0, \forall i$ (see Figs. 1, 3b); and,

(iii) the system is swung-up and is required to perform one complete revolution around the fixed pivot O before coming to rest again in the upside-down 'inverted pendulum' position with all the hinges again aligned vertically above the pivot O so that $\theta_i^{final} = 3\pi, \dot{\theta}_i^{final} = 0, \forall i$.

In Fig. 3, the black dot at the bottom indicates the position of the pivot O at which the pendulum system is connected to its fixed base of support (see Fig. 1 also). The vertical diamond shows the tip of the last (10^{th}) body, and the other dots indicate the locations of other hinges. The dashed line indicates the line going through the hinges.

The equation of motion (29) of the controlled system, with Q^C explicitly specified by relation (36), is integrated in the abovementioned three cases using ode15s using a relative error tolerance of 10^{-7} and an absolute tolerance of 10^{-9}. Each simulation is run for 25 s.

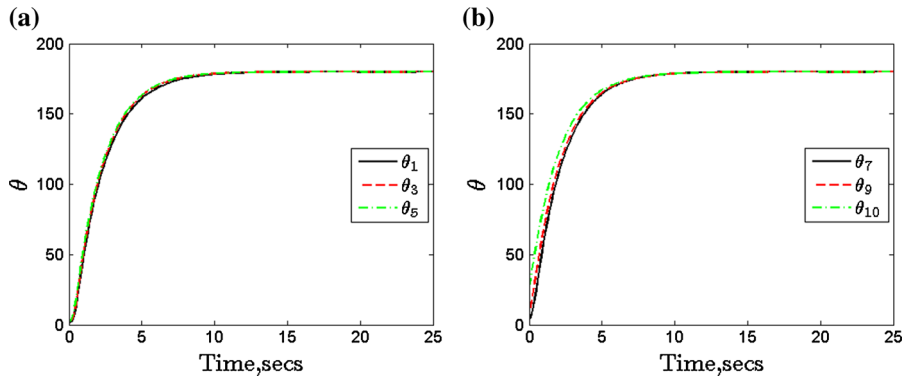

Fig. 4 Case (i). Variation of angles (degrees) with time. **a** θ_i, $i = 1, 3, 5$. **b** θ_i, $i = 7, 9, 10$

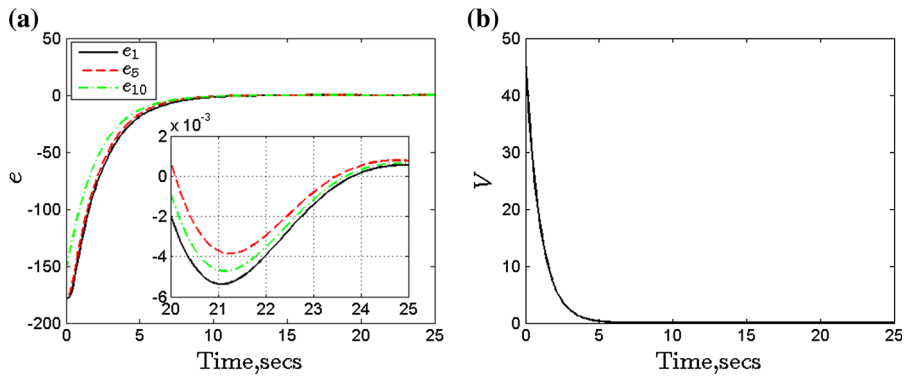

Fig. 5 Case (i). **a** Variation of errors e_i=$(\theta_i - \theta_i^{final})$, i = 1, 5, 10 (degrees) with time. **b** Variation of Lyapunov function V with time

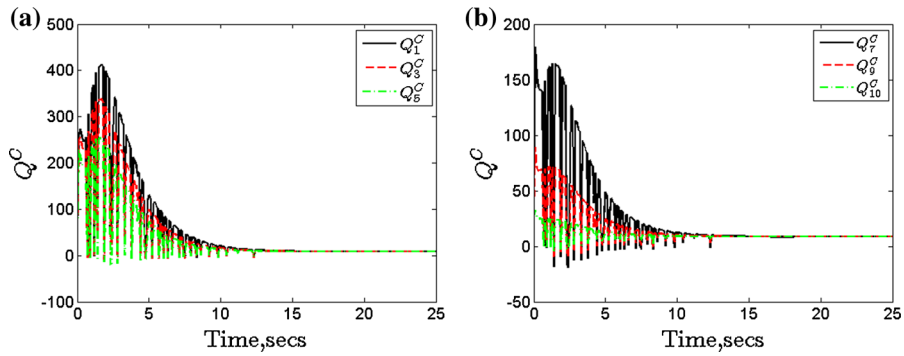

Fig. 6 Case (i). Variation of control torques (N-m) with time. **a** Q_i^C, $i = 1, 3, 5$. **b** Q_i^C, $i = 7, 9, 10$

Figure 4a shows the results of the simulation for Case (i) in which the angles θ_i, $i = 1, 3, 5$, are plotted as functions of time; Figure 4b similarly shows the variation in the angles θ_i, $i = 7, 9, 10$. Figure 5a shows the errors $e_i = (\theta_i - \theta_i^{final})$, $i = 1, 5, 10$. The inset plot shows these errors over the time interval from 20 to 25 secs; as seen, the errors are of the order of 10^{-3}. For brevity, in what follows we do not show plots for $\theta_i = 2, 4, 6,$ and 8. Figure 5b shows the variation of the Lyapunov function with time. Figure 6a shows the control torques (in N-m) required to be applied at the first, third, and fifth hinges, while Figure 6b shows those needed at the seventh, ninth, and tenth hinges. Though the control Q^C is a continuous function of time, as seen from these figures, it resembles a kind of bang-bang control in the initial part of the time history. The final position of the inverted pendulum at the end of this simulation is shown in Fig. 3a.

Figures 7, 8, and 9 similarly show results for the swing-up described in case (ii) above in which the final state is a stable position with $\theta_i^{final} = 5\pi/4$, $\dot{\theta}_i^{final} = 0, \forall i$. The final position acquired by the 10-body pendulum at the end of the simulation is shown in Fig. 3b.

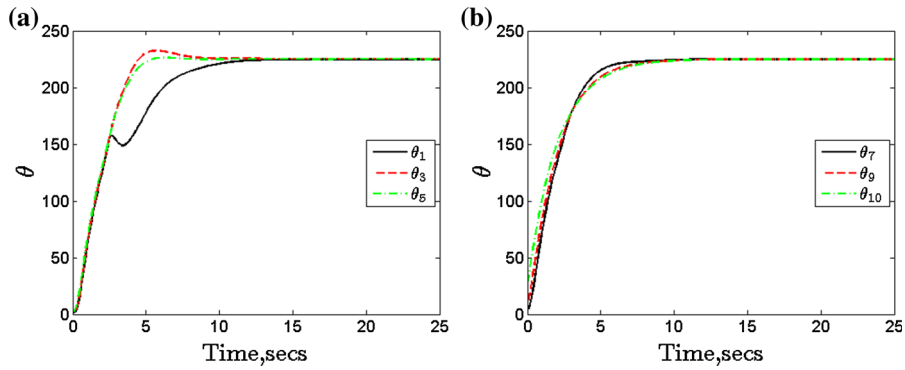

Fig. 7 Case (ii). Variation of angles (degrees) with time. **a** θ_i, $i = 1, 3, 5$. **b** θ_i, $i = 7, 9, 10$

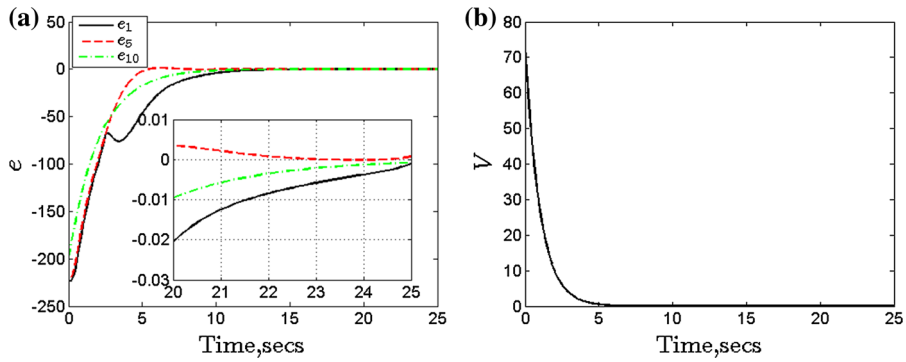

Fig. 8 Case (ii). **a** Variation of errors e_i, $i = 1, 5, 10$, with time. **b** Variation of Lyapunov function V with time

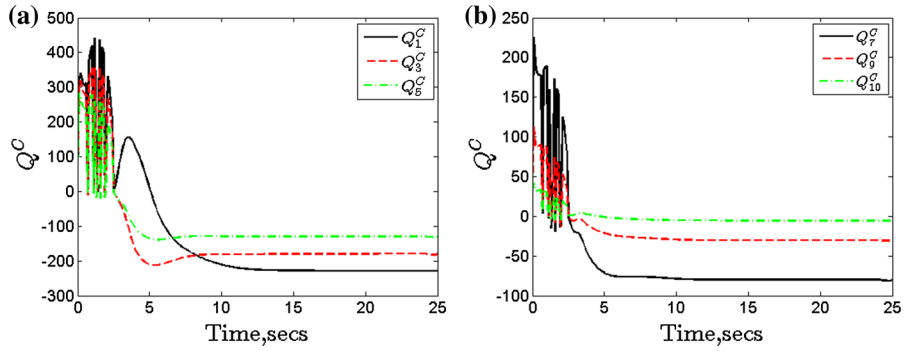

Fig. 9 Case (ii). Variation of control torques (N-m) with time. **a** Q_i^C, $i = 1, 3, 5$. **b** Q_i^C, $i = 7, 9, 10$

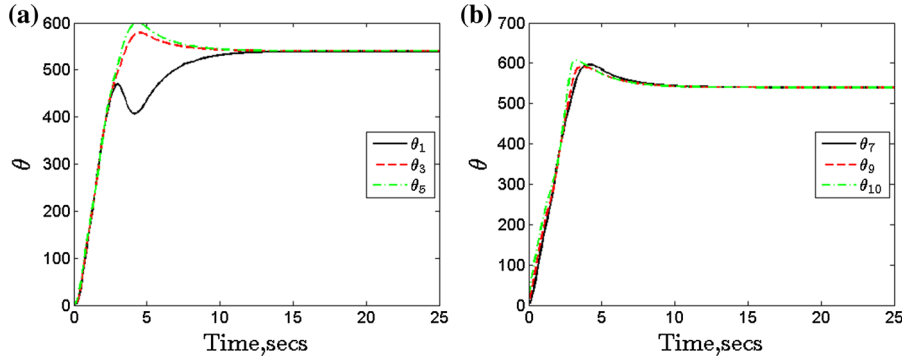

Fig. 10 Case (iii). Variation of angles (degrees) with time. **a** θ_i, $i = 1, 3, 5$. **b** θ_i, $i = 7, 9, 10$

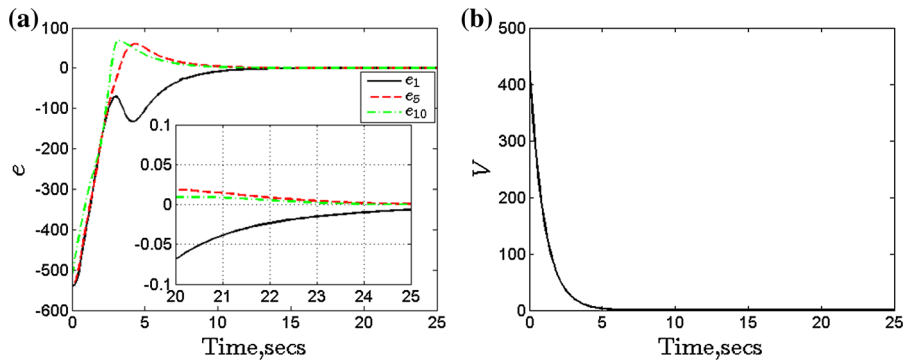

Fig. 11 Case (iii). **a** Variation of errors e_i, $i = 1, 5, 10$, with time. **b** Variation of Lyapunov function V with time

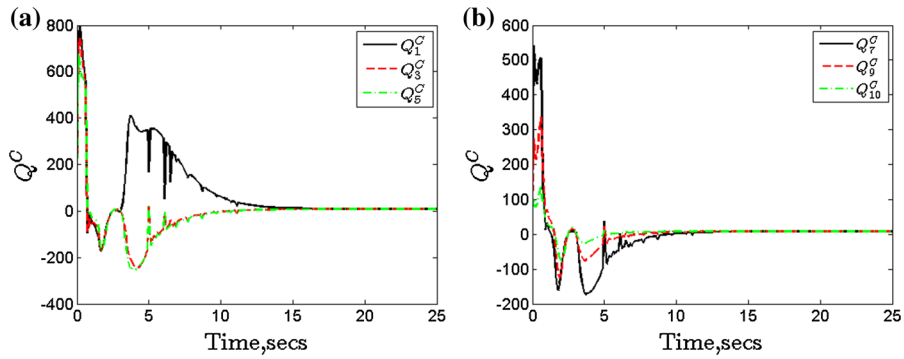

Fig. 12 Case (iii). Variation of control torques (N-m) with time. **a** Q_i^C, $i = 1, 3, 5$. **b** Q_i^C, $i = 7, 9, 10$

Figure 10 shows the changes in θ_i with time for case (iii) wherein the pendulum system makes one complete revolution about the fixed pivot before coming to rest in its final 'inverted' state. The final position of the pendulum is shown in Fig. 3a. Figure 11a shows the errors $e_i = (\theta_i - \theta_i^{final})$, $i = 1, 5, 10$, and Fig. 11(b) shows the change in the Lyapunov function with time. Figure 12 shows the requisite control torques that need to be applied to the corresponding hinges as functions of time for achieving this.

We note that since the Lyapunov function given in Eq. (35) is radially unbounded, the explicit control given in Eq. (36) is, theoretically speaking, globally stable.

4 Control of an uncertain *n*-body pendulum system

4.1 Sliding mode controller for uncertain pendulum system

In the previous section, it was assumed that the various parameters that specify the characteristics of the pendulum system are all perfectly known. However, in practical situations, there is always an uncertainty in our knowledge of the system. Control of the pendulum system in which all its parameters are not precisely known is explored in this section. For example, values of the dimensions of the various bodies comprising the system, and/or values of the mass of each body (and therefore the density of the material of each body), and/or values of the damping coefficients are usually known with only certain (and often different) degrees of certainty.

Our best estimates of these parameters for a given particular pendulum system are of course available to us (often by an educated guess). From here on, the actual pendulum system—in which some or all of its parameters may be known only imprecisely—will be referred to as the 'actual system.' The system with our best estimate/assessment of its description (and its parameter values) will be called the 'nominal system.' Control of the nominal system (whose parameters are known) is dealt with in Sect. 3.1 and demonstrated in Sect. 3.2. But if these nominal control torques are to be applied on the actual system, one might not get the desired result because the actual system is different from the nominal system; in fact, the control could even drive the system unstable. One way of approach-

ing this problem is through the use of an additional controller that ensures that the controlled actual system tracks the trajectories of the controlled nominal system. This additional controller needs to be robust, and hence, sliding mode control is a natural choice because of its robustness against norm-bounded uncertainties [21,22]. However, there are a few well-documented disadvantages associated with discontinuous sliding mode control, like, possible damage to actuators due to high frequency switching, excitation of unmodeled dynamics [22,23], and the presence of 'chatter.' The higher-order sliding mode (HOSM) method [24] attempts to address some of these problems by using a higher-dimensional sliding manifold consisting of higher-order derivatives of the sliding variable. But it has the disadvantage that the controller needs the knowledge of the higher-order derivatives of the state variable which are not always readily available and/or reliably measureable. A quite different approach from the above is taken in Ref. [25] for systems that admit two Lyapunov functions whose null sets only have a trivial intersection. A limitation of this approach is that it requires certain assumptions on the system including the assumption that the controlled system has continuous solutions and that the control does not exhibit intense chattering.

References [26] and [27] provide alternate control methodologies that also take into account model uncertainties. They differ from the approach presented herein in the following aspects: (i) While control of the nominal system in [26] and [27] is of the PD-type, the control obtained herein for the nominal system is derived from a user-defined Lyapunov function and its specified rate of decay; no a priori structure (e.g., PD) on the controller is imposed, and use is made of recent results from analytical dynamics instead of conventional control theory [15–17]. More importantly, this control *simultaneously* minimizes a user-specified quadratic control cost at *each* instant of time [6]. The control methods developed in [26] and [27] do not simultaneously minimize a user-prescribed control cost; they simply provide stable controllers. (ii) The additional control that takes care of the uncertainty in the system's description in this paper is simpler in that different expressions are not required to evaluate this additional control inside and outside the so-called bounding region. In fact, the additional controller in this paper causes the dynamics to never leave the bounding region. Also, the controller used herein is neither discontinuous, nor does it use regularization (to make it continuous), nor any saturation function.

A continuous controller has been proposed in Ref. [28] using the concept of generalized sliding surfaces where uncertainties in both the parameters describing the system and in the given forces are included. In this approach, a user supplied smooth function is utilized in the control design instead of the signum function that is traditionally used in sliding mode control methods. This control methodology has been successfully applied for nonlinear decentralized systems [29] and formation-keeping control of satellite systems under uncertainty [30]. However, in this approach, the maximum allowable uncertainty in the system parameters reduces as the number of degrees of freedom of the system increases. Hence, it is not well suited for large systems with significant uncertainties in their system parameters.

In the current work, an additional controller is designed to compensate for the uncertainties in the actual system wherein the maximum allowable uncertainties do not depend on the number of degrees of freedom of the system. This additional controller ensures that the controlled actual system tracks the trajectories of the nominal system within user-specified error bounds. Since the nominal system and the actual system start out with the same initial conditions, the tracking errors in the generalized position and generalized velocity start within these error bounds and stay within them thereafter. Thus, the actual system always remains in an attracting region around the trajectory of the nominal system; this attracting region can be specified by the user and made arbitrarily small. The approach presented in Ref. [28] is modified to obtain the controller developed here. Instead of a user supplied smooth function in the control design as in Ref. [28], attention is focused here on the use of a linear function.

The equation of motion of the controlled 'actual' n-body pendulum system is

$$M_a(\theta_a)\ddot{\theta}_a = Q_a(\theta_a, \dot{\theta}_a) + Q^C(t) + Q^u(\theta_a, \dot{\theta}_a). \quad (37)$$

The subscript 'a' under various quantities denotes that they refer to the actual system. The nominal control force is shown here as only a function of time; it does not depend on the state of the actual system. Its dependence is only on the state of the nominal system as shown in Eq. (34). Q^u is the additional generalized control force applied to the actual system, which is not known precisely, so it can track the nominal sys-

tem within a certain error bound. In what follows, the method to compute Q^u will be described. Details of the proof are provided in the Appendix.

Since uncertainties in the mass of a mechanical system have perhaps the most pervasive effect on its response, we consider below the situation wherein the uncertainty in our description of the pendulum system resides in our lack of exact knowledge of the mass of each body, or alternately, of the density of the material of which each body of the pendulum is made.

The tracking error between the actual and the nominal system is

$$e_a(t) = \theta_a(t) - \theta(t), \dot{e}_a(t) = \dot{\theta}_a(t) - \dot{\theta}(t). \tag{38}$$

where $(\theta, \dot{\theta})$ is the state of the nominal system. A sliding surface is defined as,

$$s(t) = \dot{e}_a(t) + k e_a(t) \tag{39}$$

where $k > 0$ is an arbitrary positive number. When the actual system can be restricted to stay on the sliding surface $s = 0$, it tracks the trajectories of the nominal system exactly, since they both start out with same initial conditions. However, since we intend to use a smooth function (instead of the signum function that is used traditionally), we can only ensure that the actual system stays within a small region around the origin, $s \in \Omega_\varepsilon$. This region Ω_ε, defined as

$$\Omega_\varepsilon := \left\{ s \in R^n \,|\, \|s\| \leq \varepsilon \right\}, \tag{40}$$

can be made arbitrarily small, as will be seen shortly.

On defining,

$$\delta\ddot{q} = M_a^{-1}(Q_a + Q^C) - M^{-1}(Q + Q^C), \tag{41}$$

where M is the mass matrix of the nominal system, the method requires the computation of the following estimates,

$$\text{(i)} \quad \lambda_{\min} := \min\{eigenvalues \text{ of } M_a^{-1}\}, \tag{42}$$

$$\text{(ii)} \quad \beta \geq \frac{\|\delta\ddot{q}\| + k\,\|\dot{e}\|}{\lambda_{\min}}, \forall t \quad . \tag{43}$$

In the above relations, $\|\cdot\|$ denotes the L_2 norm. Having obtained these quantities, the simple closed-form expression for the additional control force is given as,

$$Q^u = -\beta(s/\varepsilon). \tag{44}$$

In this expression, ε is a positive number, which can be chosen by the user so as to meet desired tracking tolerances. The tracking errors are guaranteed to be within the bounds given by (for a Proof, see the Appendix),

$$|e_{a,i}| \leq \frac{1}{k}\varepsilon, |\dot{e}_{a,i}| \leq 2\varepsilon, i = 1, 2, \cdots, n. \tag{45}$$

Thus, as seen from the above equation, decreasing the value of ε has the effect of shrinking the region Ω_ε and reducing the maximum possible errors in tracking.

Remark 4 It must be noted that the Lyapunov constraint (Eq. 30) is no longer strictly satisfied by the controlled actual system described by Eq. (37). However, the controlled response, at each instant of time, remains in a small region around the response of the nominal system, and this region can be made arbitrarily small.

Remark 5 In the preceding discussion, we have assumed that there is no uncertainty in the measurement of the initial conditions of the actual system. Were such an uncertainty to exist, then all the arguments made in the Appendix would go through for the controller described by Eqs. (42)–(44) to show that the region Ω_ε will be asymptotically attracting. The error estimates given in Eq. (45) will now be valid asymptotically.

4.2 Numerical example

A 10-body pendulum system is again considered. The nominal system—our best guess of the actual system—is identical to the one laid out in Sect. 3.2. The mass of each body of the nominal system is 6.28 kg. If the uncertainty in the measurement of the mass of each body is about 0.1kg, this will result in about a 1.6% discrepancy in the calculation of the mass density of the material, or about 125 kg/m^3. In what follows, the maximum possible error in the estimate of the density of each body is conservatively taken to be 150 kg/m^3.

For the purpose of demonstrating the efficacy of the control approach, ten samples are drawn from a uniform distribution of density over the range $7,850 \pm 150$ kg/m^3 for each of the ten bodies of the actual 10-body pendulum system. The densities of these bodies (correct to two decimal places) starting from the first to the tenth are, respectively, 7863.02, 7783.51, 7827.35, 7953.44, 7701.41, 7736.47, 7901.23, 7947.76, 7741.01, and 7872.53 kg/m^3. It is important to note that these specific density values are used only to demonstrate the effectiveness of the control approach; the control method would work for all other possible values of the densities that lie in this specified range. The other parameters describing the 10-body pendulum system are the same as those given in Sect. 3.2. Thus, the mass of the ith body of the actual system is $0.08 t_h \rho_{a,i}$

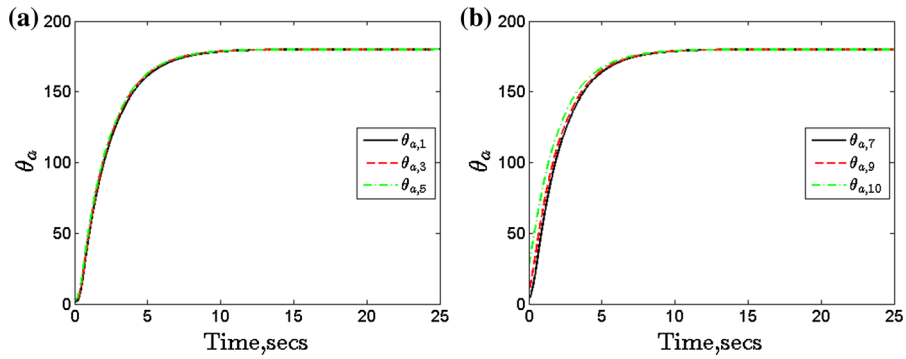

Fig. 13 Case (i). Variation of angles (degrees) of the actual pendulum with time. **a** $\theta_{a,i}$, $i = 1, 3, 5$. **b** $\theta_{a,i}$, $i = 7, 9, 10$

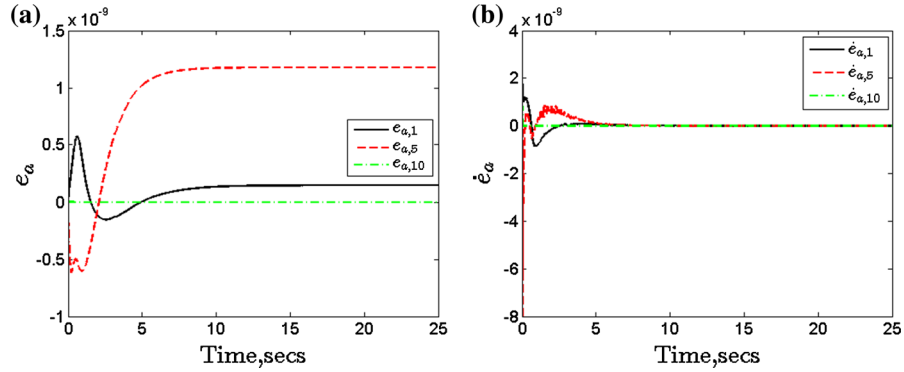

Fig. 14 Case (i). Variation of the error in tracking the nominal system with time **a** $e_{a,i}$, $i = 1, 5, 10$. **b** $\dot{e}_{a,i}$, $i = 1, 5, 10$

and its moment of inertia about its center of mass is $0.002833 t_h \rho_{a,i}$, where $\rho_{a,i}$ is the density of the ith body. The value of the thickness of each body, t_h, is taken to be 0.01m as before.

This uncertainty in the density leads to uncertainties in the mass and the mass moment of inertia of each individual body. This ultimately leads to uncertainties in the system's response that are not just confined to the mass matrix, M_a, in Eq. (37) but indeed percolate into the force vector, Q_a, of the pendulum system as well.

The equation of motion of the controlled nominal system is,

$$M\ddot{\theta} = Q + Q^C, \tag{46}$$

where the nominal generalized control force Q^C is computed using Eq. (36). The equation of motion of the controlled actual system is,

$$M_a\ddot{\theta}_a = Q_a + Q^C + Q^u \tag{47}$$

where the additional control torque Q^u is computed using Eq. (44). We choose the parameters for the additional controller to be $\varepsilon = 10^{-4}, k = 10$. Estimating conservatively $\|\delta\ddot{q}\|$ to be of $O(10^2)$ over the duration of the simulation, and $\lambda_{\min}$ and $\|\dot{e}\|$ to be of $O(10^{-3})$, we choose $\beta = 10^5$. For these chosen parameters, we are guaranteed that the tracking errors in position and velocity as given by Eq. (45) are,

$$|e_{a,i}| \leq \frac{1}{k}\varepsilon = 10^{-5}, |\dot{e}_{a,i}| \leq 2\varepsilon = 2 \times 10^{-4}, \quad i = 1, 2, \cdots, n. \tag{48}$$

Equations (46) and (47) are numerically integrated simultaneously using the ode15s package on the MATLAB platform. The relative and absolute tolerances for integration are chosen to be 10^{-7} and 10^{-10}, respectively.

Computations for the three cases simulated in Sect. 3.2 are again carried out in which the actual pendulum system starts from rest in its static stable equilibrium position and is required to come to rest so that (i) $\theta_{a,i}^{final} = \pi, \forall i$, (ii) $\theta_{a,i}^{final} = 5\pi/4, \forall i$, and, (iii) $\theta_{a,i}^{final} = 3\pi, \forall i$. Recall, the subscript 'a' denotes the actual system.

Figures 13, 14 and 15 deal with Case (i). Figure 13a shows the results of the simulation in which the angles $\theta_{a,i}, i = 1, 3, 5$, of the actual system are plotted as functions of time; Fig. 13b similarly shows the variation in the angles $\theta_{a,i}, i = 7, 9, 10$. These can be compared with similar figures for the nominal system shown in Fig. 4a, b. Figure 14a shows the error

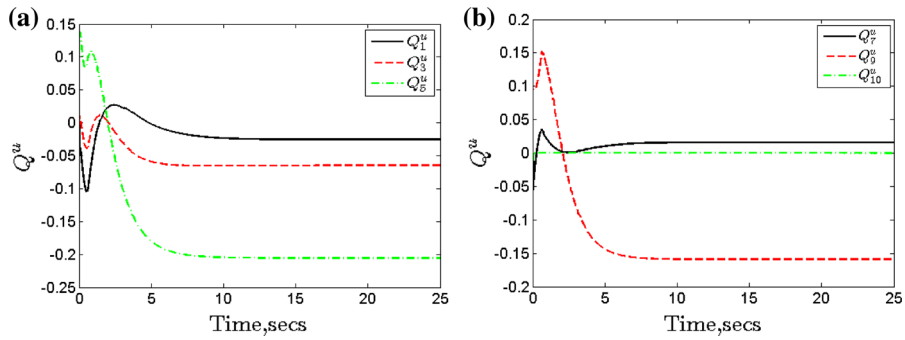

Fig. 15 Case (i). Additional control torques (N-m) on the hinges as a function of time. **a** $Q_i^u, i = 1, 3, 5$. **b** $Q_i^u, i = 7, 9, 10$

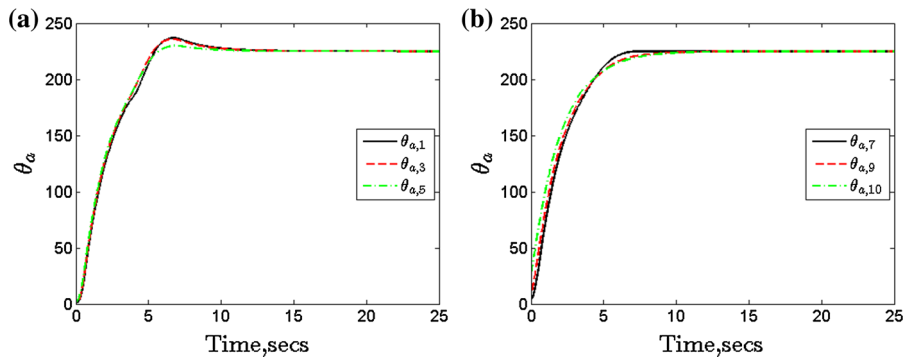

Fig. 16 Case (ii). Variation of angles (degrees) of the actual pendulum with time. **a** $\theta_{a,i}, i = 1, 3, 5$. **b** $\theta_{a,i}, i = 7, 9, 10$

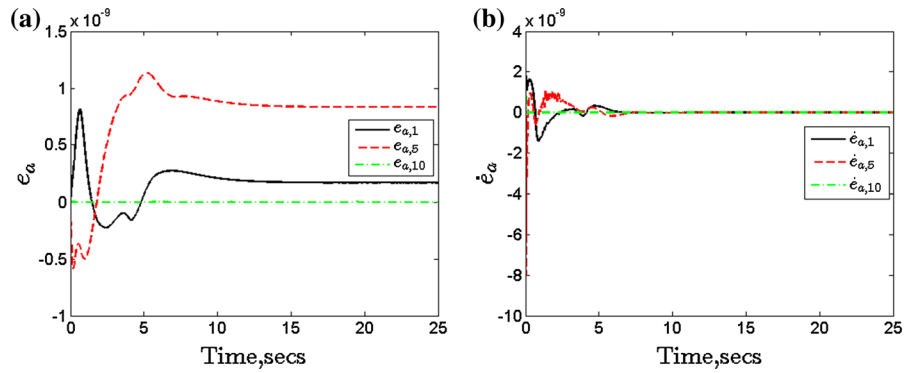

Fig. 17 Case (ii). Variation of the error in tracking the nominal system with time. **a** $e_{a,i}, i = 1, 5, 10$. **b** $\dot{e}_{a,i}, i = 1, 5, 10$

$e_{a,i} = (\theta_{a,i} - \theta_i), i = 1, 5, 10$, in tracking the nominal system, and Fig. 14b shows the error in tracking the (generalized) velocity $\dot{e}_{a,i} = (\dot{\theta}_{a,i} - \dot{\theta}_i), i = 1, 5, 10$, of the nominal system. These values are seen to be much smaller than the bounds of 10^{-5} and 2×10^{-4} guaranteed (see Eq. (48)) due to our choice of the parameter ε. Figure 15a shows the additional control torques required to be applied at the first, third, and fifth hinges, while Fig. 15b shows those applied at the seventh, ninth, and tenth hinges. It is seen that the additional control torques needed to compensate for uncertainty in our knowledge of the system are small when compared to those found for the nominal system (see Fig. 6).

Figure 19a shows the variation of the Lyapunov function with time. As mentioned in Remark 4, the Lyapunov function of the actual system is not guaranteed to satisfy Eq. (30). But since the trajectories of the actual system lie within a tight region around the nominal system, the plot for the time history of the Lyapunov function V for the actual system looks almost exactly the same as that for the nominal system (compare Fig. 19a with Fig. 5b). The rate of decay of the Lyapunov function and hence the rate of convergence of the system to the desired equilibrium point can be tuned by increasing or decreasing the parameter α.

Figures 16, 17, and 18 similarly show results for the swing-up described in the second case in which

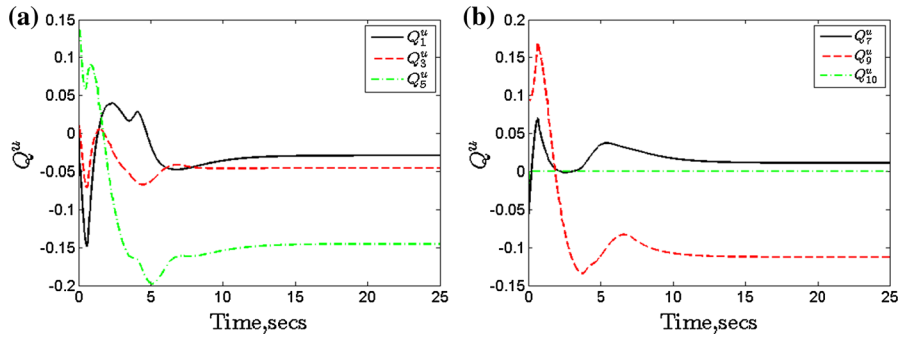

Fig. 18 Case (ii). Additional control torques (N-m) on the hinges as a function of time. **a** $Q_i^u, i = 1, 3, 5$. **b** $Q_i^u, i = 7, 9, 10$

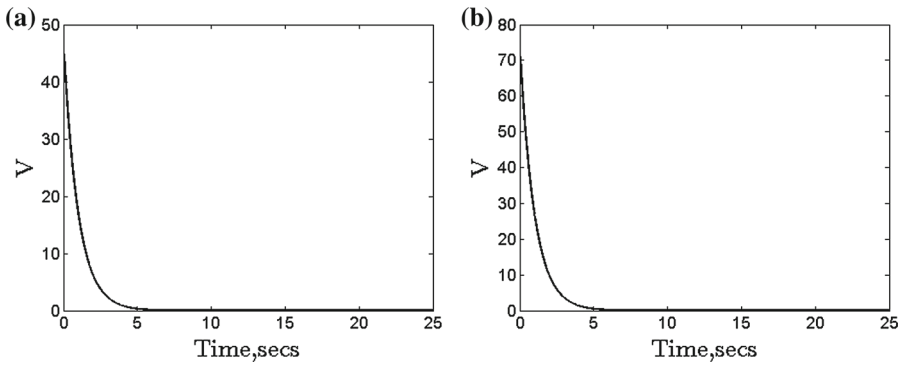

Fig. 19 Variation of Lyapunov function for the actual system with time. **a** Case (i). **b** Case (ii)

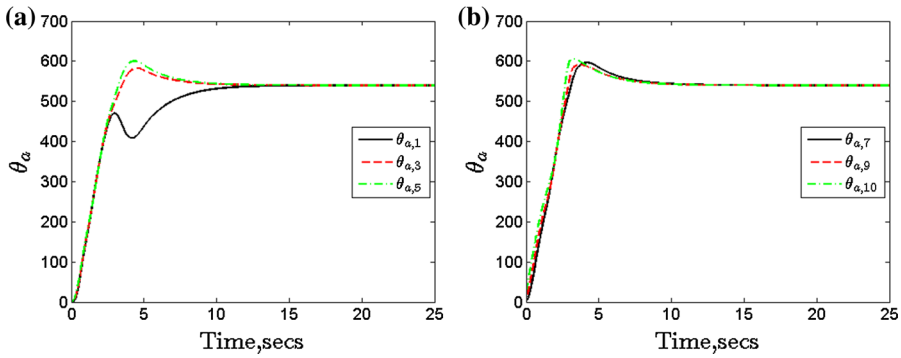

Fig. 20 Case (iii). Variation of angles (degrees) of the actual pendulum with time. **a** $\theta_{a,i}, i = 1, 3, 5$. **b** $\theta_{a,i}, i = 7, 9, 10$

the final state is a (stable) position with $\theta_{a,i}^{final} = 5\pi/4, \dot{\theta}_{a,i}^{final} = 0, \forall i$. Figure 16a shows the time history of angles of the actual system $\theta_{a,i}, i = 1, 3, 5,$, and Fig. 16b shows the same for angles $\theta_{a,i}, i = 7, 9, 10$. These can be compared with corresponding figures for the nominal system, 7(a), 7(b). Figure 17a and b show the tracking errors in the generalized position and velocity for the first, fifth, and tenth body. The tracking errors are found to be much smaller than the prescribed values of 10^{-5} and 2×10^{-4}. Figure 18a shows the time histories of additional control torques applied at the first, third, and, fifth hinges of the actual system. Figure 18b shows the same for the seventh, ninth, and tenth hinges. These additional torques are also small when compared with the nominal torques shown in Fig. 6a and b. Figure 19b shows the plot of Lyapunov function for this case. Again, the plot looks closely like the one in Fig. 8b.

Figures 20, 21, and 22 show the corresponding plots for Case (iii) in which the desired final state is at $\theta_{a,i}^{final} = 3\pi, \dot{\theta}_{a,i}^{final} = 0, \forall i$. The response of the actual pendulum system is shown in Fig. 20a, b. These plots can be compared with the corresponding plots for the nominal system in Fig. 10a and b. Figure 21a and b shows the variation in the tracking errors with time and it is again seen to be much smaller than the values predicted by theoretical analysis. Figure 22a and b shows the additional control torques that, when applied

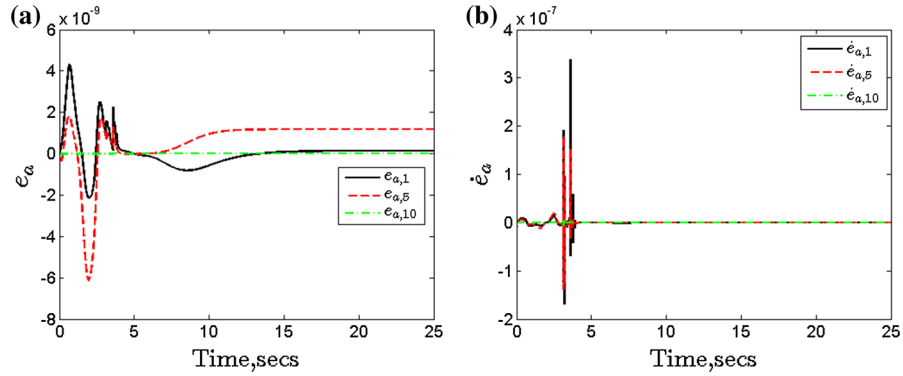

Fig. 21 Case (iii). Variation of the error in tracking the nominal system with time. **a** $e_{a,i}$, $i = 1, 5, 10$. **b** $\dot{e}_{a,i}$, $i = 1, 5, 10$

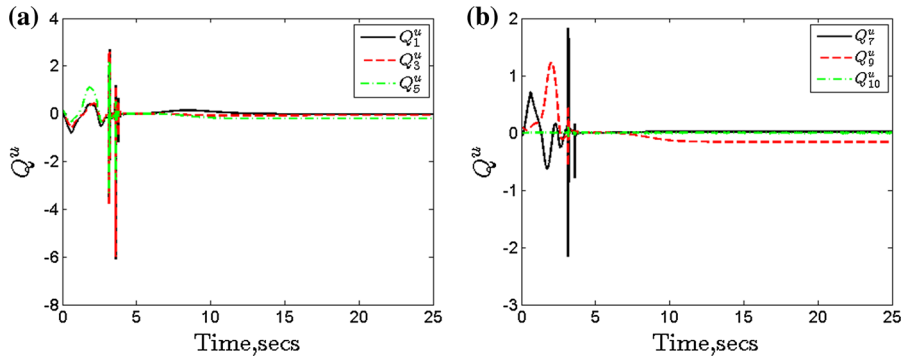

Fig. 22 Case (iii). Additional control torques (N-m) on the hinges as a function of time. **a** Q^u_i, $i = 1, 3, 5$. **b** Q^u_i, $i = 7, 9, 10$

in conjunction with the control torques shown in Fig. 12a and b, stabilize the controlled actual system to a small region around the desired equilibrium position. The plot of the Lyapunov function for this case is very similar to the plot for the corresponding nominal system (Fig. 11b) and is not shown. In all the three cases, the controlled actual system closely tracks the trajectories of the nominal system, thus satisfying the control objective. Also, the additional control torques needed to compensate for the uncertainty in the knowledge of the actual system are small compared with the control torques needed to control the nominal system.

5 Conclusions

The salient contributions of this paper are the following.

(1) It demonstrates the use of mathematical induction to derive the equations of motion for an n-body planar pendulum system in a compact form. This method simplifies the procedure for obtaining the equations of motion by significantly reducing the (near-exponentially increasing) algebraic complexity involved in their derivation. The center of mass of each body comprising the n-body pendulum system is not assumed to lie on a straight line joining the hinges, as is the common practice in the literature hereto. Hence, the equations are more general than those hereto reported in the literature, and they provide a better approximation to reality.

(2) In the case when the properties of the system are assumed to be perfectly known—the nominal system—a simple control method inspired by analytical dynamics is suggested for controlling the nonlinear system to drive it to any desired final state. The method is different from those based on conventional control theory. It makes no simplifying assumptions/linearizations related to the nonlinear dynamical system; nor does it impose any a priori structure on the nature of the nonlinear controller. The approach makes use of the fundamental equation of mechanics that enforces a user-prescribed Lyapunov constraint on the system to obtain an explicit expression for the control force. An important feature of the control so obtained is that it simultaneously minimizes a user-specified quadratic control cost at each instant of time. Through a proper choice of the Lyapunov function, the control can be made globally asymptotically stable.

(3) Further, when the parameters of the system are known with bounded uncertainty, an additional continuous controller is used, which forces the controlled system to track the trajectories of the nominal system within user-prescribed bounds. This ensures that the controlled actual (uncertain) system is stable in the sense that it is asymptotically attracted to a region, which can be made arbitrarily small, around the desired equilibrium point. This additional continuous controller, though substantially different from that proposed in Ref. [28], is inspired partly by the generalized sliding surface controller developed there.

(4) Numerical examples are provided showing the simplicity and efficacy of the control methodology. A nonlinearly damped 10-body pendulum whose description may or may not be precisely known is considered. This system has a substantially larger number of degrees of freedom than those reported to date in the literature. Each body in the pendulum is taken to be L-shaped. The pendulum starts from its static equilibrium position and is 'swung-up' in a controlled fashion to be brought to rest so that it remains in various 'inverted positions.' Stable (optimal) control of the nominal system and the actual (uncertain) system are demonstrated. Global asymptotic control of the nonlinear system is achieved.

This paper illustrates the power of analytical dynamics. Its use provides novel ways of controlling highly nonlinear dynamical systems without making any simplifying assumptions/linearizations regarding either the description of system's dynamics or the structure of the controller. It is interesting that by using the theory of constrained motion of mechanical systems closed-form robust controllers can be designed with considerable ease, thereby yielding a simple methodology for nonlinear control that has perhaps been overlooked thus far. Finally, we point out that the approach used here can be easily extended to other complex dynamical systems.

6 Appendix

In this section, the proofs for the results regarding the additional controller used in Sect. 4 are provided. For convenience, we recall the following.

The equation of motion of the controlled nominal system is

$$M(\theta)\ddot{\theta} = Q(\theta, \dot{\theta}) + Q^C(t). \tag{49}$$

The equation of motion of the controlled actual system is

$$M_a(\theta_a)\ddot{\theta}_a = Q_a(\theta_a, \dot{\theta}_a) + Q^C(t) + Q^u(\theta_a, \dot{\theta}_a). \tag{50}$$

In the above equation, the additional (generalized) control force Q^u is computed using the expression

$$Q^u = -\beta(s/\varepsilon) \tag{51}$$

where ε is a small positive number, s is the sliding variable

$$s := \dot{e}_a + ke_a, \quad k > 0, \tag{52}$$

and β is a positive number satisfying the condition

$$\beta \geq \frac{\|\delta\ddot{q}\| + k\,\|\dot{e}_a\|}{\lambda_{\min}}, \forall t, \text{ where}$$
$$\lambda_{\min} := \min\{eigenvalues \text{ of } M_a^{-1}\}. \tag{53}$$

In Eq. (53), $\delta\ddot{q}$ is a quantity defined as,

$$\delta\ddot{q} := M_a^{-1}(Q_a + Q^C) - M^{-1}(Q + Q^C), \tag{54}$$

and $\|.\|$ represents L_2 norm of a vector.

Result 1: The additional control force Q^u given by

$$Q^u = -\beta(s/\varepsilon) \tag{55}$$

where ε is a small positive number and β is a positive number satisfying the condition given in Eq. (53) ensures that the controlled actual system

$$M_a(\theta_a)\ddot{\theta}_a = Q_a(\theta_a, \dot{\theta}_a) + Q^C(t) + Q^u(\theta_a, \dot{\theta}_a). \tag{56}$$

stays with in the region Ω_ε defined by

$$\Omega_\varepsilon := \left\{s \in R^n \,|\, \|s\| \leq \varepsilon\right\}. \tag{57}$$

Proof Noting the definition of the sliding manifold in Eq. (52), its derivative with respect to time is,

$$\dot{s}(t) = \ddot{e}_a + k\dot{e}_a. \tag{58}$$

Upon differentiating the tracking error $e_a(t) = \theta_a(t) - \theta(t)$ twice, we have

$$\ddot{e}_a(t) = \ddot{\theta}_a(t) - \ddot{\theta}(t). \tag{59}$$

Using the equations of motion of the controlled nominal system (Eq. 49) and the controlled actual system (Eq. 56), Eq. (59) becomes

$$\ddot{e}_a = M_a^{-1}(Q_a + Q^C) - M^{-1}(Q + Q^C) + M_a^{-1}Q^u$$
$$= \delta\ddot{q} + M_a^{-1}Q^u. \tag{60}$$

The last equality above is obtained from the definition of $\delta\ddot{q}$ in Eq. (54). Thus, the time derivative of the sliding manifold can be simplified using Eq. (60) as,

$$\dot{s}(t) = \ddot{e}_a + k\dot{e}_a = \delta\ddot{q} + M_a^{-1}Q^u + k\dot{e}_a. \tag{61}$$

Considering the Lyapunov function

$$V_a = \frac{1}{2}s^T s, \tag{62}$$

its rate of change along the trajectories of the dynamical system is given by

$$\begin{aligned}\dot{V}_a &= s^T\dot{s}\\ &= s^T(\delta\ddot{q} + M_a^{-1}Q^u + k\dot{e}_a)\\ &= s^T(\delta\ddot{q} - M_a^{-1}\beta\left(\frac{s}{\varepsilon}\right) + k\dot{e}_a).\end{aligned} \tag{63}$$

Observing that $s^T M_a^{-1} s \geq \lambda_{\min}\|s\|^2$, we have

$$\begin{aligned}\dot{V}_a &\leq \|s\|\,\|\delta\ddot{q}\| + k\|s\|\,\|\dot{e}_a\| - \beta\lambda_{\min}\frac{\|s\|^2}{\varepsilon}\\ &= \|s\|\left(\|\delta\ddot{q}\| + k\|\dot{e}_a\| - \beta\lambda_{\min}\frac{\|s\|}{\varepsilon}\right).\end{aligned} \tag{64}$$

The region Ω_ε is defined such that $\|s\| \leq \varepsilon$, and we have $\|s\|/\varepsilon > 1$ outside Ω_ε. Hence outside Ω_ε, the right-hand side of Eq. (64) is strictly negative when $\beta \geq \frac{\|\delta\ddot{q}\|+k\|\dot{e}_a\|}{\lambda_{\min}}$. Since the controlled actual system starts inside the region Ω_ε, it stays within this attracting region and cannot escape from it. □

As pointed out in Remark 5, if the nominal system and the uncertain system do not start with the same initial conditions, then any trajectories of the controlled uncertain system that start from outside Ω_ε are globally attracted to the region Ω_ε.

Result 2: If the controlled actual system is restricted to stay within the region Ω_ε, the errors in tracking the nominal system are bounded by,

$$|e_{a,i}| \leq \frac{1}{k}\varepsilon, |\dot{e}_{a,i}| \leq 2\varepsilon, i = 1, 2, \cdots, n. \tag{65}$$

Proof Inside the region Ω_ε, $\|s\| \leq \varepsilon$ and hence,

$$|s_i| \leq \varepsilon, i = 1 \cdots n. \tag{66}$$

From the relation $s_i = \dot{e}_{a,i} + ke_{a,i}$, we get,

$$|\dot{e}_{a,i} + ke_{a,i}| \leq \varepsilon, i = 1 \cdots n. \tag{67}$$

This inequality can be alternatively expressed as,

$$-\varepsilon \leq \dot{e}_{a,i} + ke_{a,i} \leq \varepsilon, \tag{68}$$

which can further be simplified to

$$-\varepsilon - ke_{a,i} \leq \dot{e}_{a,i} \leq \varepsilon - ke_{a,i}. \tag{69}$$

Considering $e_{a,i}$ as a dynamical system, if we can prove that $e_{a,i}\dot{e}_{a,i} < 0$ (which is the derivative of the Lyapunov function $\frac{1}{2}e_{a,i}e_{a,i}$) outside a region L_ε^i, we can conclude that the region L_ε^i is an attracting region. Defining L_ε^i as,

$$L_\varepsilon^i := \left\{e_{a,i} \in R | \left|e_{a,i}\right| \leq \frac{1}{k}\varepsilon\right\}, \tag{70}$$

there are two possible cases in which $e_{a,i}$ could lie outside L_ε^i. Let us look at both of them.

Case 1: If $e_{a,i} > \frac{1}{k}\varepsilon > 0$, then $\varepsilon - ke_{a,i} < 0$. From Eq. (69), we then have

$$e_{a,i}\dot{e}_{a,i} \leq e_{a,i}\left(\varepsilon - ke_{a,i}\right) < 0. \tag{71}$$

Case 2: If $e_{a,i} < -\frac{1}{k}\varepsilon < 0$, then $\varepsilon + ke_{a,i} < 0$. Also, $e_{a,i} < 0$ and so from the left inequality in (69), we have,

$$e_{a,i}\dot{e}_{a,i} \leq -e_{a,i}\left(\varepsilon + ke_{a,i}\right) < 0. \tag{72}$$

We note that initially $e_{a,i} = 0$, and therefore, it will remain inside the region L_ε^i thereafter, or in other words, $\left|e_{a,i}\right| \leq \frac{1}{k}\varepsilon$. From relation (67), we observe that

$$\left|\left|\dot{e}_{a,i}\right| - \left|ke_{a,i}\right|\right| \leq \left|\dot{e}_{a,i} + ke_{a,i}\right| \leq \varepsilon, \tag{73}$$

which further yields

$$\left|\dot{e}_{a,i}\right| \leq \varepsilon + \left|ke_{a,i}\right| \leq 2\varepsilon. \tag{74}$$

□

References

1. Eltohamy, K.H., Kuo, C.-Y.: Nonlinear generalized equations of motion for multi-link inverted pendulums. Int. J. Syst. Sci. **30**, 505–515 (1999)
2. Larcombe, L.J.: On the control of two-dimensional multi-link inverted pendulum: the form of the dynamic equations from choice of co-ordinate system. Int. J. Syst. Sci. **23**, 2265–2289 (1992)
3. Lobas L. G.: Generalized Mathematical Model of an Inverted multi-link Pendulum with Follower Forces, **41**(5), pp. 566–572, (2005)
4. Lobas, L.G.: Dynamic behaviour of multi-link pendulums under follower forces. Int. Appl. Mech. **41**(6), 587–613 (2005)
5. Cheng, P.-Y., Cheng-I, W., Chen, C.-K.: Symbolic derivation of dynamic equations of motion for robot manipulators using piogram symbolic method. IEEE J. Rob. Autom. **4**(6), 599–609 (1988)

6. Udwadia, F. E.: A new approach to stable optimal control of complex nonlinear dynamical systems. J. Appl. Mech. **81**(3), (2013)
7. Çimen T.: State-dependent Riccati equation (SDRE) control: a survey. In: Proceedings of the 17th world congress, IFAC, Seoul, Korea, July 6–11, (2008)
8. Sontag, E.D.: A universal construction of Artstein's theorem on nonlinear stabilization. Syst. Control Lett. **13**(2), 117–123 (1989)
9. Freeman, R.A., Koktovic, P.V.: Inverse optimality in robust stabilization. SIAM J. Control Optim. **34**, 1365–1392 (1996)
10. Khalil, H.K.: Nonlinear Systems. Prentice Hall, New Jersey (2002)
11. Krstic, M., Kanellakopoulos, I., Kokotovic, P.V.: Nonlinear and Adaptive Control Design. Wiley, New York (1995)
12. Åström, K.J., Furuta, K.: Swinging up a pendulum by energy control. Automatica **36**, 287–295 (2000)
13. Ibáñez, C.A., Azuela, J.H.S.: Stabilization of the Furuta pendulum based on a Lyapunov function. Nonlinear Dyn. **49**, 1–8 (2007)
14. Ibáñez, C.A., Castanon, M.S., Cortés, N.C.: Output feedback stabilization of the inverted pendulum system: a Lyapunov approach. Nonlinear Dyn. **70**, 767–777 (2012)
15. Udwadia, F.E.: Analytical Dynamics. Cambridge University Press, Cambridge (2008)
16. Udwadia, F.E., Kalaba, R.E.: A new perspective on constrained motion. Proc. R. Soc. Lond. Ser. A **439**, 407–410 (1992)
17. Udwadia, F.E., Kalaba, R.E.: What is the general form of explicit equations of motion for constrained mechanical systems? J. Appl. Mech. **69**(3), 335–339 (1992)
18. Udwadia, F.E.: A new perspective on the tracking control of nonlinear structural and mechanical systems. Proc. R. Soc. Lond. Ser. A **459**, 1783–1800 (2003)
19. Udwadia, F.E.: Optimal tracking control of nonlinear dynamical systems. Proc. R. Soc. Lond. Ser. A **464**, 2341–2363 (2008)
20. Udwadia, F.E., Schutte, A.D.: A unified approach to rigid body rotational dynamics and control. Proc. R. Soc. Lond. Ser. A **468**, 395–414 (2012)
21. Utkin, V.I.: Sliding modes and their application in variable structure systems. Mir Publishers (English Translation). Moscow, Russia (1978)
22. Young, K.D., Utkin, V.I., Özgüner, Ü.: A control engineer's guide to sliding mode control. IEEE Trans. Control Syst. Technol. **7**(3), 328–342 (1999)
23. Spurgeon, S.K.: Sliding mode observers: a survey. Int. J. Syst. Sci. **39**(8), 751–764 (2008)
24. Levant, A.: Higher-order sliding modes, differentiation and output-feedback control. Int. J. Control **76**(9/10), 924–941 (2003)
25. Qu, Z., Dorsey, J.F.: Robust control by two Lyapunov functions. Int. J. Control **55**(6), 1335–1350 (1992)
26. Qu, Z.: Asymptotic stability of controlling uncertain dynamical systems. Int. J. Control **59**(5), 1345–1355 (1994)
27. Corless, M.: Control of uncertain nonlinear systems. J. Dyn. Syst. Meas. Control **115**, 362–372 (1993)
28. Udwadia, F. E., Wanichanon, T.: Control of uncertain nonlinear multibody mechanical systems. J. Appl. Mech. **81**(4), 041020 (2014)
29. Udwadia, F.E., Koganti, P.B., Wanichanon, T., Stipanović, D.M.: Decentralized control of nonlinear dynamical systems. Int. J. Control **87**(4), 827–843 (2014)
30. Udwadia, F.E., Wanichanon, T., Cho, H.: Methodology for satellite formation-keeping in the presence of system uncertainties. J. Guid. Control Dyn. **37**(5), 1611–1624 (2014)